Supporting information

Preparation of polysubstituted imidazole frames using AC-SO_3H/$[Urea]_7[ZnCl_2]_2$ as efficient catalysts system: A novel method, and α-glucosidase inhibitors activity

Hai Truong Nguyen,[a,b] Vy Anh Truong,[a,b] and Phuong Hoang Tran[a,b] *

[a] Department of Organic Chemistry, Faculty of Chemistry, University of Science, Vietnam National University, Ho Chi Minh City 700000, Viet Nam.

[b] Vietnam National University, Ho Chi Minh City 700000, Viet Nam

Email: thphuong@hcmus.edu.vn

Table of contents

Section S1. Chemicals, supplies, and instruments

Chemicals and supplies

Benzil (98%), nitrobenzene (99%), 2-hydroxybenzaldehyde (99%), 3-hydroxybenzaldehyde (99%), 3-methoxy-4-hydroxybenzaldehyde (99%), 4-hydroxybenzaldehyde (98%), 4-bromobenzaldehyde (99%), 4-(dimethylamino)benzaldehyde (grade ACS reagent, 99%), cyclohexanecarboxaldehyde (97%), 4-nitrophenol (99%), 4-fluorobenzaldehyde (99%), and furfural (99%) were obtained from Sigma-Aldrich. Benzaldehyde (for synthesis), 4-nitrobenzaldehyde (for synthesis), 4-methylbenzaldehyde (for synthesis), 4-methoxybenzaldehyde (for synthesis), ammonium acetate (for synthesis), zinc chloride ($ZnCl_2$) (for analysis), iron powder, ammonium chloride (for synthesis), ethanol (for synthesis), choline chloride (for synthesis), glycerine (for synthesis), dichloromethane (for synthesis), 1,4-dioxane (for synthesis), sulfonic acid (for synthesis), TLC (silica gel 60 F254), and silica gel 230–400 mesh (for column chromatography) were obtained from Merck. Ethyl acetate (purity ≥ 99.5%), *n*-hexane (purity ≥ 99.5%), and chloroform (purity ≥ 99%) were obtained from Xilong Chemical. Co., Ltd (China). *α*-Glucosidase (EC 3.2.1.20) from *Saccharomyces cerevisiae* (750 UN) and *p*-nitrophenyl-*α*-*d*-glucopyranoside were obtained from Sigma Chemical Co. (St. Louis, MO, USA). Acarbose and dimethylsulfoxide were purchased from Merck (Darmstadt, Germany).

Analytical techniques

Merck silica gel (60, 230-400 mesh) was used in column chromatography. The 1H and 13C NMR spectra were taken using a Bruker Avance 500 MHz. The solvent used was DMSO-d6, and the internal standards were either TMS or solvent peaks. Calculating boiling points included using the Buchi melting point B-545. A Bruker E400 FT-IR spectrometer was used to measure the Fourier transforms infrared (FT-IR) spectra. ATR-FTIR spectra between 400 and 600 cm-1. The Q-500 thermal gravimetric analyzer was used to measure TGA, with a temperature ramp of 5 °C/min and airflow. On a Bruker D8 Advance, powder X-ray diffraction (P-XRD) data were obtained using Ni-filtered Cu K (λ= 1.54059) radiation. Using the Hitachi S-4800 scanning electron microscope and the XZS-107T digital microscope connected to NHV-CAM via the program eScope, the materials' morphology was examined (SEM). The Quantachrome NOVA 3200e system was used to quantify the N2 isotherm at 77 K. To ascertain the elemental composition of sorbents, energy-dispersive X-ray spectroscopy (EDX) examination was performed utilizing an EMAX energy EX-400 EDX instrument.

Section S2. General procedure

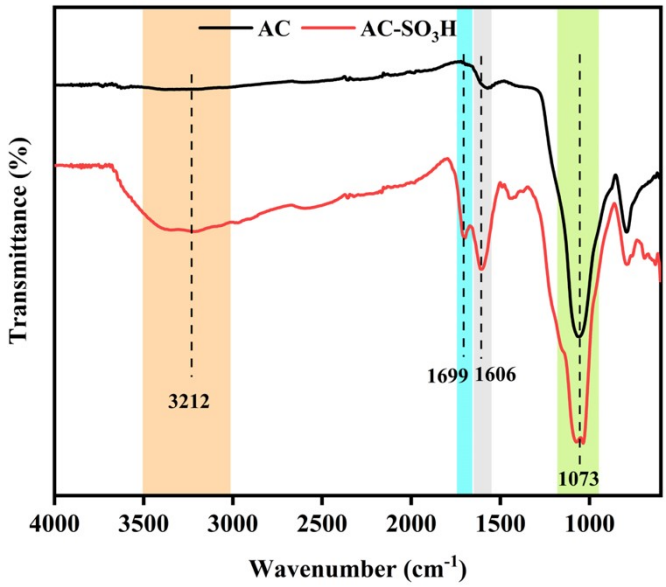

Fig. S1. FT-IR spectrum of AC and AC-SO_3H.

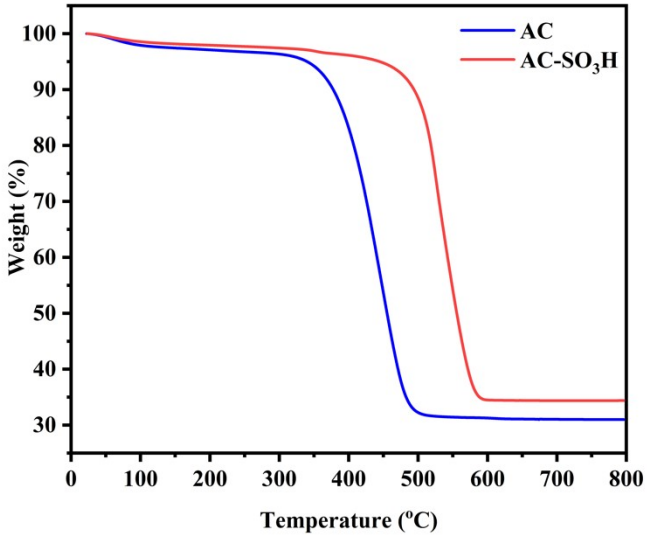

Fig. S2. TGA of AC and AC-SO_3H.

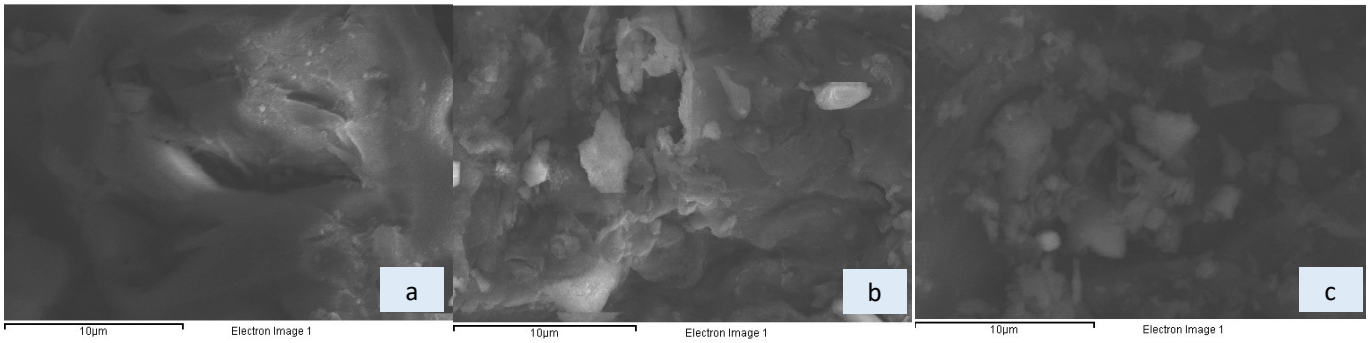

Fig. S3. SEM image of AC, AC-SO_3H, and AC-SO_3H (after 4 times).

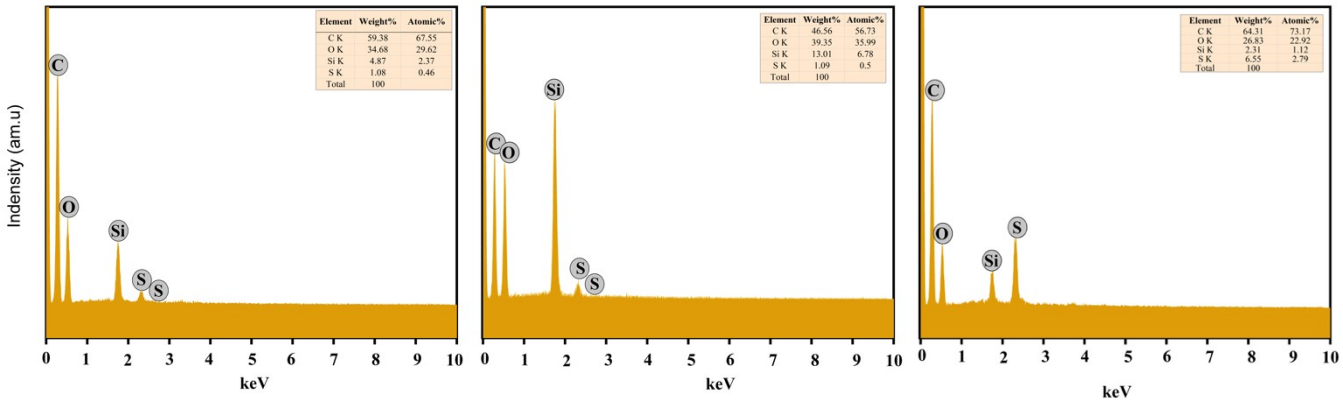

Fig. S4. EDX analysis of AC, AC-SO_3H, and AC-SO_3H (after 4 times).

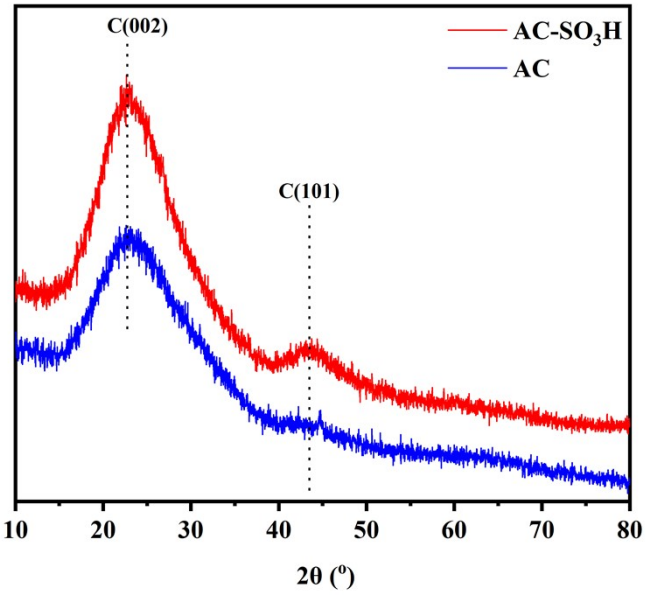

Fig. S5. P-XRD analysis of AC and AC-SO_3H.

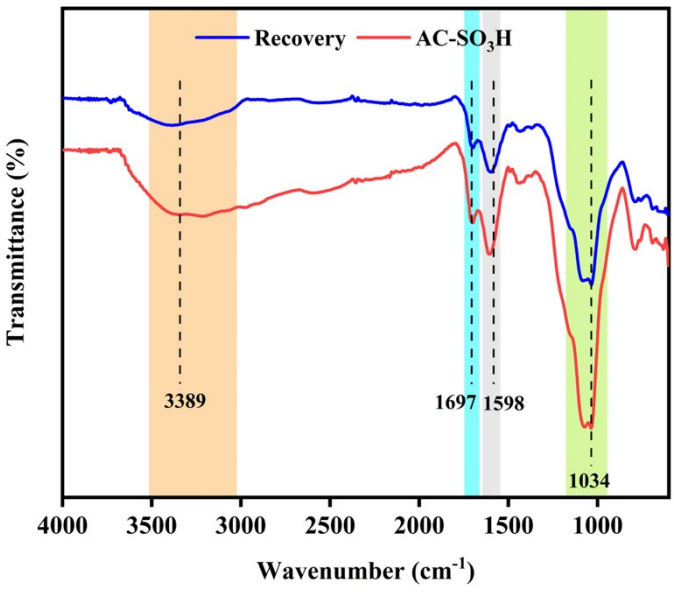

Fig. S6. FT-IR of AC-SO_3H and AC-SO_3H (after 4 times).

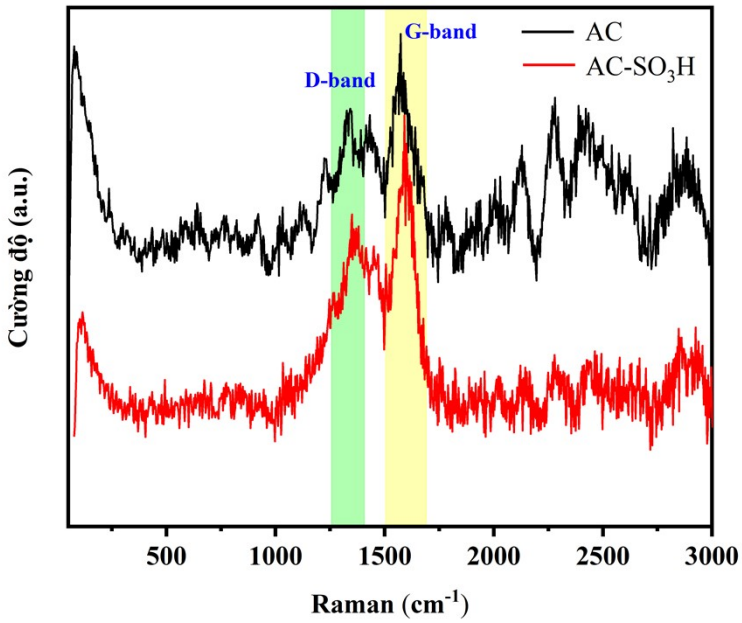

Fig. S7. Raman of AC and AC-SO_3H

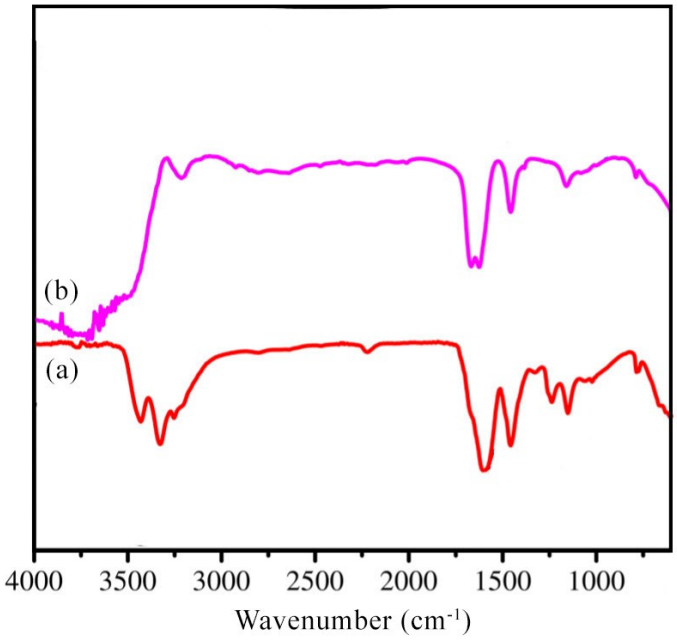

Fig. S8. FT-IR of $[Urea]_7[ZnCl_2]_2$ (a), and Urea (b).

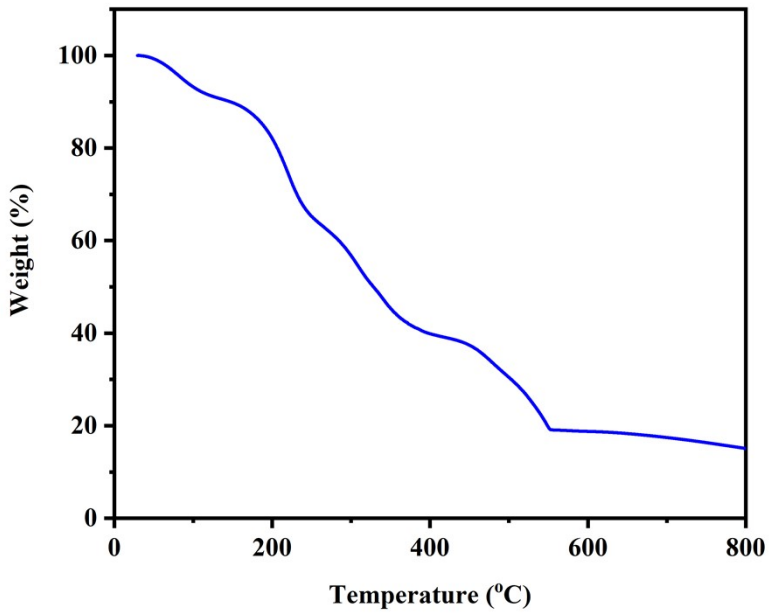

Fig. S9. TGA of $[Urea]_7[ZnCl_2]_2$

Section S3. Optimization of reaction conditions

Table S1. Optimization of the conversion of nitrobenzene to aniline.[a]

Entry	Temperature (°C)	Time (min)	Conversion[b] (%)
1	30 (RT)	60	79.41
2	60	60	100.00
3	60	15	60.04
4	60	30	81.81
5	60	45	89.85

[a]Reaction conditions: Nitrobenzene (1.0 mmol, 123 mg), ammonium chloride (1.5 mmol, 79.5 mg), and iron powder (3.0 mmol, 168 mg) under H_2O/EtOH (v/v = 1:1).

[b]Conversion was recorded by GCMS.

Table S2. Optimization of reaction conditions.[a]

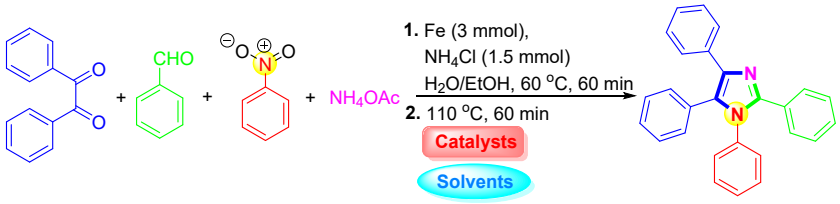

Entry	Temperature (°C)	Time (min)	Catalyst loading (mg)	Yields[b] (%)	TON	TOF (h^{-1})
1	80	60	10	20	63	63

2	100	60	10	46	144	144
3	**110**	**60**	**10**	**73**	**228**	**228**
4	130	60	10	75	234	234
5	110	30	10	36	113	113
6	110	90	10	74	231	231
7	110	60	0	43	134	134
8	110	60	1	44	138	138
9	110	60	3	51	159	159
10	110	60	5	64	200	200
11	110	60	15	61	191	191

[a]Reaction conditions: Nitrobenzene (1.0 mmol, 123 mg), ammonium chloride (1.5 mmol, 79.5 mg), and iron powder (3.0 mmol, 168 mg) under H_2O/EtOH (v/v = 1:1) at 60 ^oC for 60 min. Then, benzil (1.0 mmol, 210 mg), benzaldehyde (1.0 mmol, 106 mg), ammonium acetate (1.0 mmol, 77 mg), AC-SO_3H (mg), and $[Urea]_7[ZnCl_2]_2$ (1.0 mmol).

[b]Yields were recorded by isolated yield.

Section S4. Spectral data

1,2,4,5-Tetraphenyl-1*H*-imidazole (IMI-01)[1, 2]

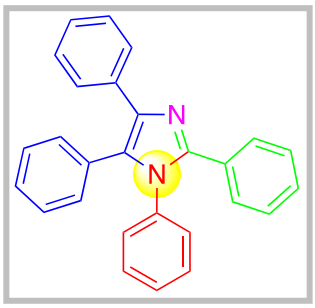

White solid, m.p = 213-217 °C

^{1}H NMR (500 MHz, $CDCl_3$) δ (ppm) 7.60 (dd, J = 8.5 Hz, 1.5 Hz, 2H), 7.43 (dd, J = 8.0, 1.5 Hz, 2H), 7.28–7.26 (m, 2H), 7.25–7.17 (m, 10H), 7.13 (dd, J = 8.0 Hz, 1.5 Hz, 2H), 7.04 (dt, J = 6.5 Hz, 1.5 Hz, 2H).

^{13}C NMR (125 MHz, $CDCl_3$) δ (ppm) 147.3, 138.7, 137.6, 134.9, 131.5, 131.3, 131.1, 131.0, 129.4, 129.4, 128.9, 128.7, 128.6, 128.6, 128.5, 128.5, 128.3, 127.8, 127.0.

LC-MS *m/z* $[M+H]^+$ 373

2-(2-Hydroxyphenyl)-1,4,5-triphenyl-1*H*-imidazole (IMI-02)[1, 3]

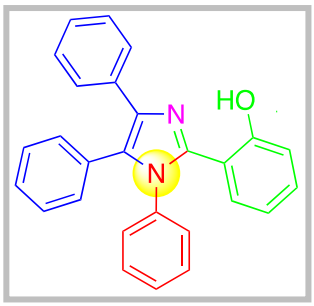

White solid, m.p = 250-254 °C

^{1}H NMR (500 MHz, DMSO-*d6*) δ (ppm) 12.57 (s, 1H), 7.45-7.26 (m, 16H), 6.94 (dd, J = 8.0 Hz, 1.0 Hz, 1H), 6.66 (dd, J = 8.0, 1.5, 1H), 6.55 (ddd, J = 8.0 Hz, 7.0 Hz, 1.0 Hz, 1H).

^{13}C NMR (125 MHz, DMSO-*d6*) δ (ppm) 157.3, 144.4, 136.6, 134.4, 133.2, 131.3, 130.8, 130.2, 129.6, 129.4, 129.3, 128.7, 128.7, 128.5, 128.4, 126.9, 126.8, 126.1, 118.1, 116.9, 113.9.

LC-MS *m/z* $[M+H]^+$ 389

2-(3-Hydroxyphenyl)-1,4,5-triphenyl-1*H*-imidazole (IMI-03)[4]

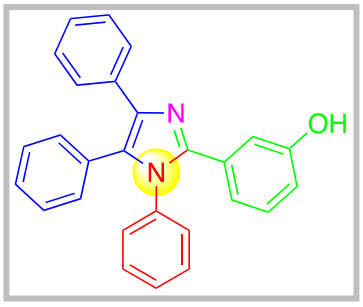

White solid, m.p = 202-205 °C

^{1}H NMR (500 MHz, DMSO-*d6*) δ (ppm) 9.47 (s, 1H), 7.48 (d, J = 7.0 Hz, 2H), 7.33-7.28 (m, 6H), 7.25–7.23 (m, 6H), 7.18–7.15 (m, 1H), 7.02 (t, J = 8.0 Hz, 1H), 6.95–6.94 (m, 1H), 6.71–6.65 (m, 1H).

^{13}C NMR (125 MHz, DMSO-*d6*) δ (ppm) 157.1, 146.1, 136.7, 136.7, 134.4, 131.5, 131.2, 131.2, 130.4, 129.1, 129.1, 128.7, 128.4, 128.4, 128.2, 126.4, 126.3, 118.9, 115.4, 115.4.

LC-MS *m/z* $[M+H]^+$ 389

2-(4-Hydroxy-3-methoxyphenyl)-1,4,5-triphenyl-1*H*-imidazole (IMI-04)[5]

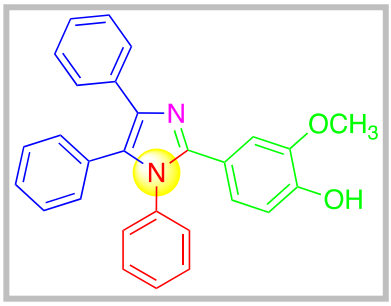

White solid, m.p = 209-210 °C

^{1}H NMR (500 MHz, $CDCl_3$) δ (ppm) 7.52–7.50 (m, 2H), 7.19–7.17 (m, 3H), 7.16–7.12 (m, 6H), 7.03 (dd, J = 8.0 Hz, 1.0 Hz, 2H), 6.95 (m, 3H), 6.76 (dd, J = 8.0 Hz, 2.0 Hz, 1H), 6.65 (d, J = 8.0 Hz, 1H), 5.65 (s, 1H), 3.61 (s, 1H).

^{13}C NMR (125 MHz, $CDCl_3$) δ (ppm) 146.9, 146.1, 146.0, 138.0, 137.4, 134.5, 131.2, 130.8, 130.5, 129.1, 128.6, 128.3, 128.2, 128.1, 127.9, 127.4, 126.6, 122.7, 122.5, 114.1, 111.8, 55.8.

LC-MS *m/z* $[M+H]^+$ 419

2-(4-Nitrophenyl)-1,4,5-triphenyl-1*H*-imidazole (IMI-05)[1, 6]

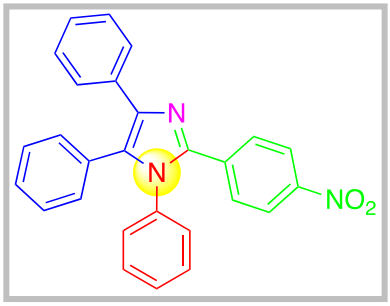

Orange solid, m.p = 194-198 °C

^{1}H NMR (500 MHz, DMSO-*d6*) δ (ppm) 8.15 (d, J = 8.5 Hz, 2H), 7.62 (d, J = 8.5 Hz, 2H), 7.51 (d, J = 7.5 Hz, 2H), 7.39-7.27 (m, 12H), 7.21 (t, J = 7.5 Hz, 1H).

^{13}C NMR (125 MHz, DMSO-*d6*) δ (ppm) 146.7, 143.8, 137.8, 136.3, 136.2, 133.9, 132.8, 131.1, 129.9, 129.5, 129.3, 128.8, 128.7, 128.6, 128.5, 128.3, 126.8, 126.4, 123.5.

LC-MS *m/z* $[M+H]^+$ 418

2-(4-Hydroxyphenyl)-1,4,5-triphenyl-1*H*-imidazole (IMI-06)[7]

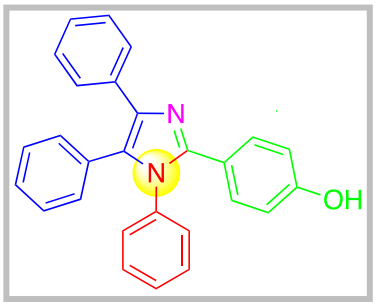

White solid, m.p = 280-283 °C

^{1}H NMR (500 MHz, DMSO-*d6*) δ (ppm) 9.67 (s, 1H), 7.47- 7.22 (m, 17H), 6.65 (s, 2H)

^{13}C NMR (125 MHz, DMSO-*d6*) δ (ppm) 157.6, 146.4, 136.9, 136.4, 134.6, 131.1, 130.6, 130.6, 129.8, 129.1, 128.8, 128.6, 128.4, 128.3, 128.1, 126.3, 121.3, 114.9.

LC-MS *m/z* $[M+H]^+$ 389

2-(4-Bromophenyl)-1,4,5-triphenyl-1*H*-imidazole (IMI-07)[8]

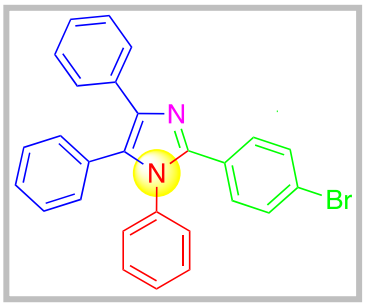

White solid, m.p = 165-168 °C

^{1}H NMR (500 MHz, DMSO-*d6*) δ (ppm) 7.50–7.47 (m, 4H), 7.34–7. 23 (m, 15H).

^{13}C NMR (125 MHz, DMSO-*d6*) δ (ppm) 157.9, 145.5, 137.3, 134.9, 132.4, 131.6, 131.6, 130.9, 130.4, 130.2, 128.9, 128.8, 128.6, 128.0, 126.9, 126.8, 122.2, 116.2.

LC-MS *m/z* $[M+H]^+$ 451

2-(4-*N*,*N*-dimethylaminophenyl)-1,4,5-triphenyl-1*H*-imidazole (IMI-08)

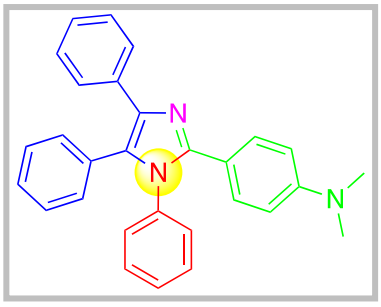

White solid, m.p =207-209 °C

^{1}H NMR (500 MHz, DMSO-*d6*) δ (ppm) 7.47 (d, J = 7.5 Hz, 2H), 7.33-7.27 (m, 7H), 7.23-7.17 (m, 8H), 6.57 (d, J = 8.5 Hz, 2H), 2.88 (s, 6H).

^{13}C NMR (125 MHz, DMSO-*d6*) δ (ppm) 149.9, 146.7, 137.1, 136.3, 134.7, 131.2, 130.7, 130.4, 129.1, 129.0, 128.8, 128.5, 128.4, 128.2, 128.1, 126.3, 126.2, 117.7, 111.3.

LC-MS *m/z* $[M+H]^+$ 416

2-(4-Methylphenyl)-1,4,5-triphenyl-1*H*-imidazole (IMI-09)[6]

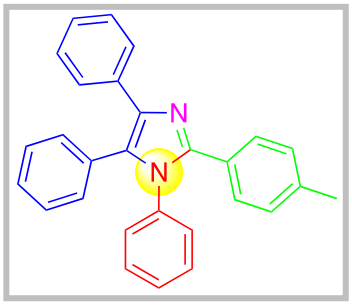

White solid, m.p = 187-190 °C

^{1}H NMR (500 MHz, DMSO-*d6*) δ (ppm) 7.50–7.47 (m, 2H), 7.33 – 7.28 (m, 6H), 7.27-7.22 (m, 9H), 7.09–7.08 (d, *J* = 8.0 Hz, 2H), 2.26 (s, 3H).

^{13}C NMR (125 MHz, DMSO-*d6*) δ (ppm) 146.1, 137.8, 136.7, 136.7, 134.5, 131.1, 131.1, 130.5, 129.1, 128.8, 128.7, 128.7, 128.4, 128.4, 128.2, 128.1, 127.6, 126.4, 126.4, 20.7.

LC-MS *m/z* $[M+H]^+$ 387

2-Cyclohexyl-1,4,5-triphenyl-1*H*-imidazole (IMI-10)

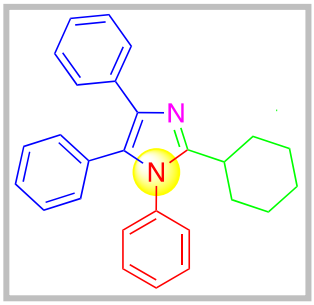

White solid, m.p = 185-186 °C

^{1}H NMR (500 MHz, DMSO-*d6*) δ (ppm) 7.54 (d, *J* = 8.5, 2H), 7.34 (m, 3H), 7.22 (t, *J* = 8, 2H), 7.11 (m, 8H), 2.50 (m, 1H), 1.86 (m, 3H), 1.78 (m, 3H), 1.64 (d, *J* = 13, 1H), 1.24 (m, 1H), 1.16 (m, 2H).

^{13}C NMR (125 MHz, DMSO-*d6*) δ (ppm) 157.7, 152.9, 135.6, 135.5, 131.6, 131.3, 130.0, 129.5, 128.8, 128.3, 128.3, 127.5, 126.7, 126.4, 116.0, 35.9, 32.2, 26.2, 25.9.

LC-MS *m/z* $[M+H]^+$ 379

2-(Furan-2-yl)-1,4,5-triphenyl-1*H*-imidazole (IMI-11)[9]

White solid, m.p = 165-167 °C

^{1}H NMR (500 MHz, DMSO-*d6*) δ (ppm) 7.66–7.64 (m, 7H), 7.37–7.31 (m, 10H).

^{13}C NMR (125 MHz, DMSO-*d6*) δ (ppm) 148.43, 138.51, 129.90, 128.60, 128.23, 126.59, 126.49.

LC-MS *m/z* $[M+H]^+$ 363

1-(4-Hydroxyphenyl)-2,4,5-triphenyl-1*H*-imidazole (IMI-12)[10-12]

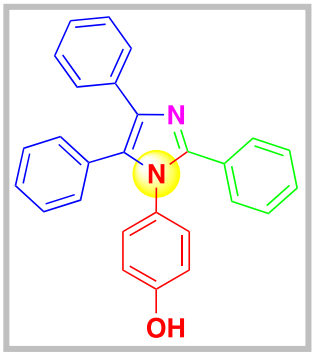

Dark reddish brown solid, m.p = 186-187 °C

^{1}H NMR (500 MHz, DMSO-*d6*) δ (ppm) 9.74 (s, 1H), 7.48 (d, J = 8.5 Hz, 2H), 7.44–7.42 (m, 2H), 7.30 (m, 6H), 7.24 (m, 4H), 7.16 (m, 1H), 7.04 (d, J = 8.5 Hz, 2H), 6.65 (d, J = 8.5 Hz, 2H).

^{13}C NMR (125 MHz, DMSO-*d6*) δ (ppm) 157.8, 146.6, 137.1, 135.0, 132.1, 131.6, 131.1, 131.1, 130.3, 128.9, 128.7, 128.6, 128.6, 128.3, 126.8, 116.1.

LC-MS *m/z* $[M+H]^+$ 389

1-(4-Hydroxyphenyl)-2-(4-hydroxyl-3-methoxyphenyl)-4,5-diphenyl-1*H*-imidazole (IMI-13)[5, 10, 13]

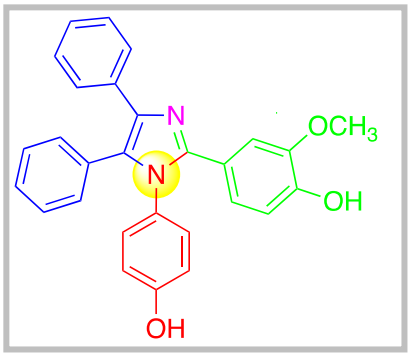

Light brown solid, m.p = 188-189 °C

^{1}H NMR (500 MHz, DMSO-*d6*) δ (ppm) 9.72 (s, 1H), 9.22 (s, 1H), 7.46 (d, J = 8.5, 2H), 7.28 (m, 3H), 7.20 (m, 4H), 7.14 (m, 1H), 7.02 (d, J = 8.5, 2H), 6.88 (m, 2H), 6.76 (m, 3H), 3.54 (s, 3H).

^{13}C NMR (125 MHz, DMSO-*d6*) δ (ppm) 157.7, 147.3, 147.3, 146.9, 136.6, 135.2, 131.6, 131.4, 131.3, 130.4, 128.9, 128.6, 128.6, 128.5, 126.8, 126.7, 122.2, 121.8, 116.0, 115.6, 112.8, 55.7.

LC-MS *m/z* $[M+H]^+$ 435

1-(4-Hydroxyphenyl)-2-(4-nitrophenyl)-4,5-diphenyl-1*H*-imidazole (IMI-14)[10, 14]

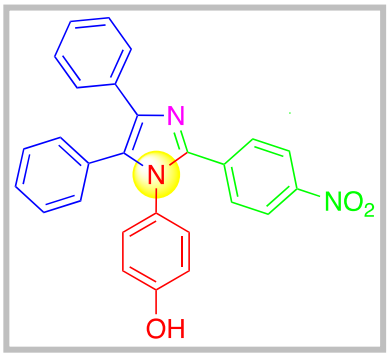

Reddish brown solid, m.p = 174-176 °C

^{1}H NMR (500 MHz, DMSO-*d6*) δ (ppm) 9.85 (s, 1H), 8.18 (d, J = 8.5, 2H), 7.69 (d, J = 8.5, 2H), 7.50 (d, J = 7.5, 2H), 7.33 (m, 3H), 7.26 (m, 4H), 7.20 (m, 1H), 7.13 (d, J = 8, 2H), 6.70 (d, J = 8.5, 2H).

^{13}C NMR (125 MHz, DMSO-*d6*) δ (ppm) 158.2, 147.1, 144.4, 138.1, 137.0, 134.5, 133.6, 131.6, 130.6, 130.2, 129.1, 129.1, 129.0, 128.7, 127.8, 127.2, 126.9, 124.0, 116.4.

LC-MS *m/z* $[M+H]^+$ 434

1,2-(4-Hydroxyphenyl)-4,5-diphenyl-1*H*-imidazole (IMI-15)[10, 15, 16]

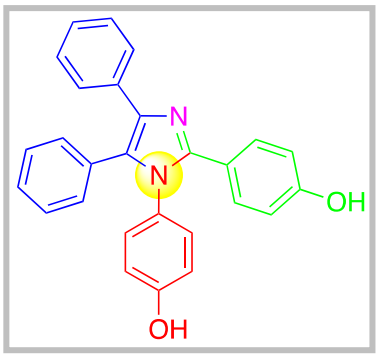

Red solid, m.p = 141-143 °C

^{1}H NMR (500 MHz, DMSO-*d6*) δ (ppm) 9.73-9.66 (d, 2H), 7.48 (d, J = 8, 2H), 7.30 (m, 3H), 7.23 (m, 6H), 7.15 (m, 1H), 7.02 (d, J = 8, 2H), 6.67 (m, 4H).

^{13}C NMR (125 MHz, DMSO-*d6*) δ (ppm) 158.0, 157.6, 147.0, 136.6, 135.2, 131.6, 131.3, 130.3, 130.1, 128.8, 128.6, 128.5, 126.8, 126.7, 122.0, 116.0, 115.4.

LC-MS *m/z* $[M+H]^+$ 405

1-(4-Hydroxyphenyl)-2-(4-methylphenyl)-4,5-diphenyl-1*H*-imidazole (IMI-16)[10, 17-19]

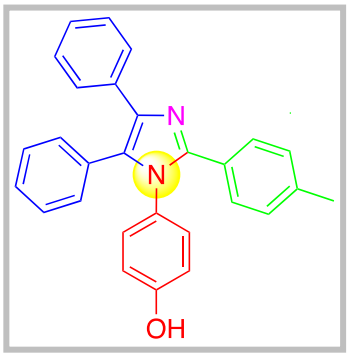

Reddish brown solid, m.p = 192-194 °C

^{1}H NMR (500 MHz, DMSO-d_6) δ (ppm) 9.73 (s, 1H), 7.48 (d, J = 8, 2H), 7.32 (m, 5H), 7.24 (m, 4H), 7.17 (m, 1H), 7.11 (d, J = 7.5, 2H), 7.04 (d, J = 8.5, 2H), 6.66 (d, J = 8.5, 2H), 2.28 (s, 3H).

^{13}C NMR (125 MHz, DMSO-d_6) δ (ppm) 157.7, 146.7, 138.1, 136.9, 135.1, 131.8, 131.6, 131.2, 130.3, 129.2, 128.8, 128.7, 128.6, 128.4, 128.3, 126.8, 126.8, 116.0, 21.2.

LC-MS *m/z* $[M+H]^+$ 403

1-(4-Hydroxyphenyl)-2-(4-bromophenyl)-4,5-diphenyl-1*H*-imidazole (IMI-17)[10]

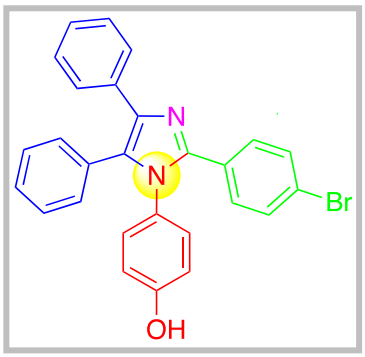

Pink solid, m.p = 129-130 °C

^{1}H NMR (500 MHz, DMSO-d_6) δ (ppm) 9.78 (s, 1H), 7.53 (d, J = 8.5, 2H), 7.48 (d, J = 8.5, 2H), 7.36 (d, J = 8.5, 2H), 7.32 (m, 3H), 7.25 (m, 4H), 7.18 (m, 1H), 7.07 (d, J = 8.5, 2H), 6.68 (d, J = 8.5, 2H).

^{13}C NMR (125 MHz, DMSO-d_6) δ (ppm) 157.7, 145.3, 137.1, 134.7, 132.2, 131.5, 131.4, 130.7, 130.3, 130.0, 130.0, 128.7, 128.7, 128.4, 127.9, 126.7, 126.6, 122.0, 116.0.

LC-MS *m/z* $[M+H]^+$ 467

1-(4-Hydroxyphenyl)-2-(4-fluorophenyl)-4,5-diphenyl-1*H*-imidazole (IMI-18)[14]

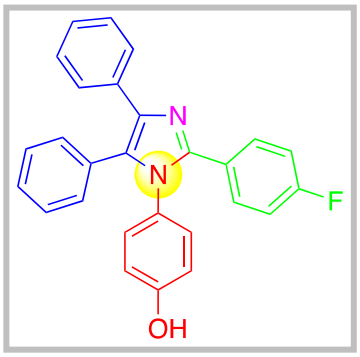

White solid, m.p = 125-126 °C

^{1}H NMR (500 MHz, DMSO-d_6) δ (ppm) 9.76 (s, 1H), 7.47 (m, 4H), 7.32 (m, 3H), 7.24 (m, 4H), 7.32 (m, 3H), 7.24 (m, 4H), 7.17 (m, 3H), 7.06 (d, J = 8.5, 2H), 6.68 (d, J = 8.5, 2H).

^{13}C NMR (125 MHz, DMSO-d_6) δ (ppm) 163.3, 161.4, 157.8, 145.7, 137.0, 135.0, 132.0, 131.6, 131.0, 130.8, 130.7, 130.3, 128.9, 128.8, 128.6, 128.1, 127.6, 126.8, 116.1, 115.7, 115.5.

LC-MS *m/z* $[M+H]^+$ 407

1-(4-Hydroxyphenyl)-2-(4-methoxyphenyl)-4,5-diphenyl-1*H*-imidazole (IMI-19)[10, 11]

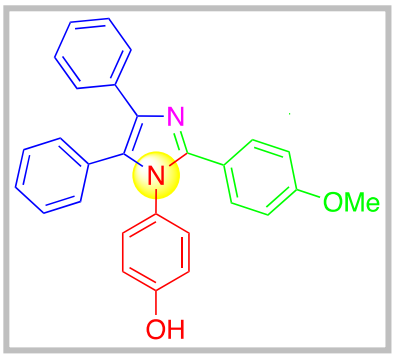

Light yellow solid, m.p = 190-191 °C

^{1}H NMR (500 MHz, DMSO-d_6) δ (ppm) 9.73 (s, 1H), 7.48 (d, J = 8.5, 2H), 7.36 (d, J = 8, 2H), 7.31 (m, 3H), 7.23 (m, 4H), 7.16 (m, 1H), 7.04 (d, J = 8.5, 2H), 6.68 (m, 2H), 6.73 (m, 2H), 3.75 (s, 3H).

^{13}C NMR (125 MHz, DMSO-d_6) δ (ppm) 159.6, 157.7, 146.6, 136.8, 135.2, 131.6, 131.3, 130.3, 130.0, 129.0, 128.8, 128.6, 128.5, 128.5, 127.4, 126.8, 126.7, 123.5, 116.1, 114.1, 55.6.

LC-MS *m/z* $[M+H]^+$ 419

1-(4-Hydroxyphenyl)-2-(4-(dimethylamino)phenyl)-4,5-diphenyl-1*H*-imidazole (IMI-20)[16]

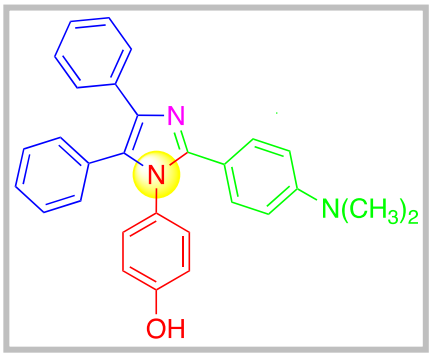

Brown solid, m.p = 179-181 °C

^{1}H NMR (500 MHz, DMSO-*d6*) δ (ppm) 10.16 (s, 1H), 7.91 (d, J = 7.5, 2H), 7.73 (m, 2H), 7.67 (m, 6H), 7.58 (m, 1H), 7.46 (d, J = 8.5, 2H), 7.11 (d, J = 8, 2H), 7.04 (d, J = 8.5, 2H), 3.79 (s, 6H).

^{13}C NMR (125 MHz, DMSO-*d6*) δ (ppm) 157.6, 150.4, 147.3, 136.6, 135.3, 131.6, 131.5, 131.2, 130.3, 129.4, 128.8, 128.5, 126.8, 126.6, 118.5, 116.1, 111.9.

LC-MS *m/z* $[M+H]^+$ 432

2-Cyclohexyl-1-(4-hydroxyphenyl)-4,5-triphenyl-1*H*-imidazole (IMI-21)

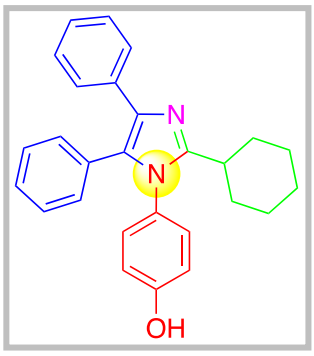

White solid, m.p = 160-161 °C

^{1}H NMR (500 MHz, DMSO-*d6*) δ (ppm) 9.74 (s, 1H), 7.42 (d, J = 8, 2H), 7.26 (m, 3H), 7.20 (t, J = 7.5, 2H), 7.16 (m, 2H), 7.12 (m, 1H), 7.08 (d, J = 8.5, 2H), 6.73 (d, J = 8.5, 2H), 2.40 (m, 1H), 1.81 (d, J = 12, 2H), 1.74 (m, 2H), 1.62 (m, 3H), 1.18 (m, 1H), 1.13 (m, 2H).

^{13}C NMR (125 MHz, DMSO-*d6*) δ (ppm) 157.7, 152.8, 135.6, 135.5, 131.6, 131.3, 130.0, 129.5, 128.8, 128.4, 128.3, 127.5, 126.7, 126.4, 126.0, 35.9, 32.2, 26.2, 25.9.

HRMS (ESI): *m/z* $[M+H]^+$ calcd for $C_{27}H_{27}N_2O^+$: 395.2123; found: 295.2132.

Section S5. ^{1}H, ^{13}C NMR, and HRMS spectroscopy

^{1}H, ^{13}C NMR spectrum of 1,2,4,5-Tetraphenyl-1*H*-imidazole (IMI-01)

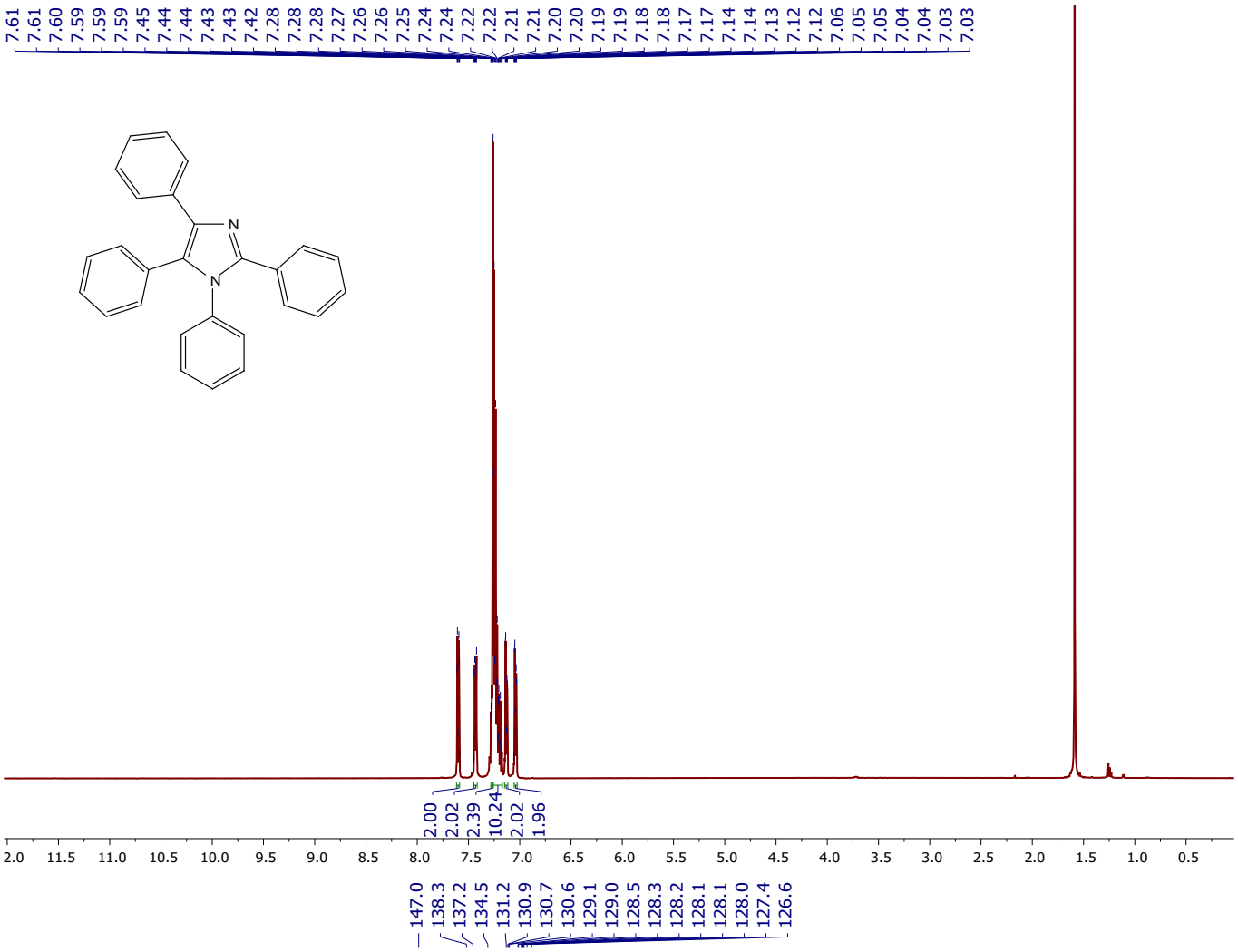

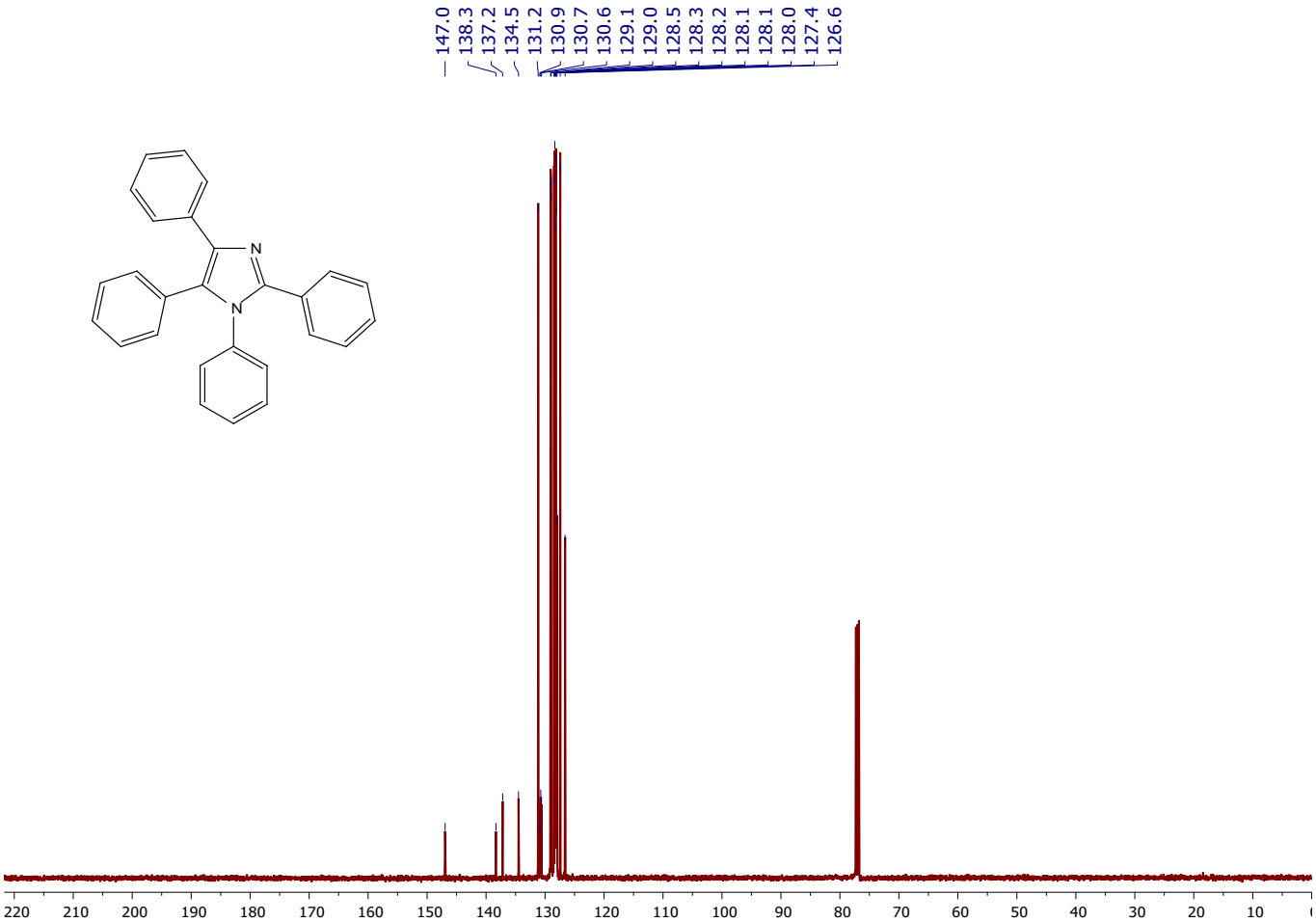

^{1}H, ^{13}C NMR spectrum of 2-(2-Hydroxyphenyl)-1,4,5-triphenyl-1*H*-imidazole (IMI-02)

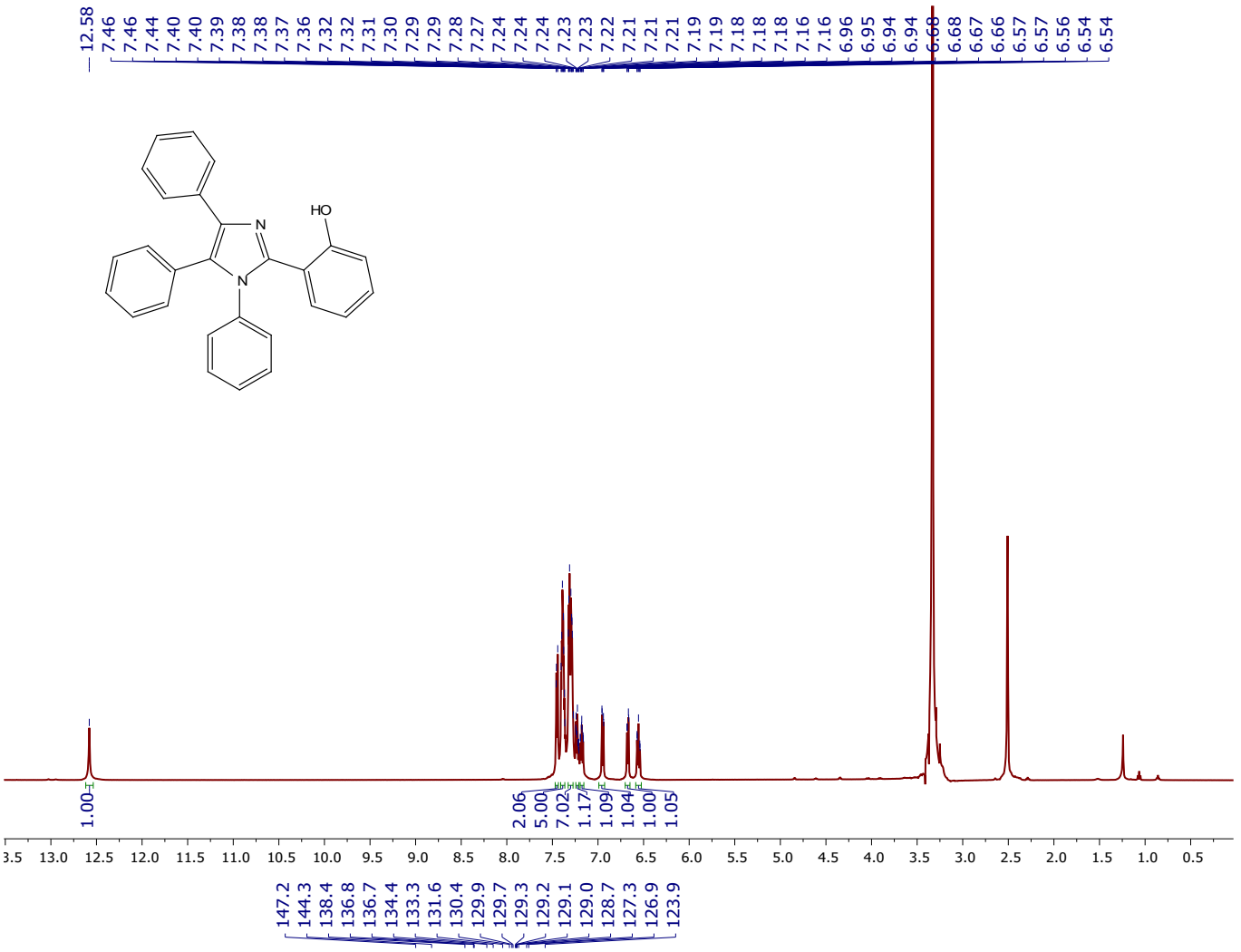

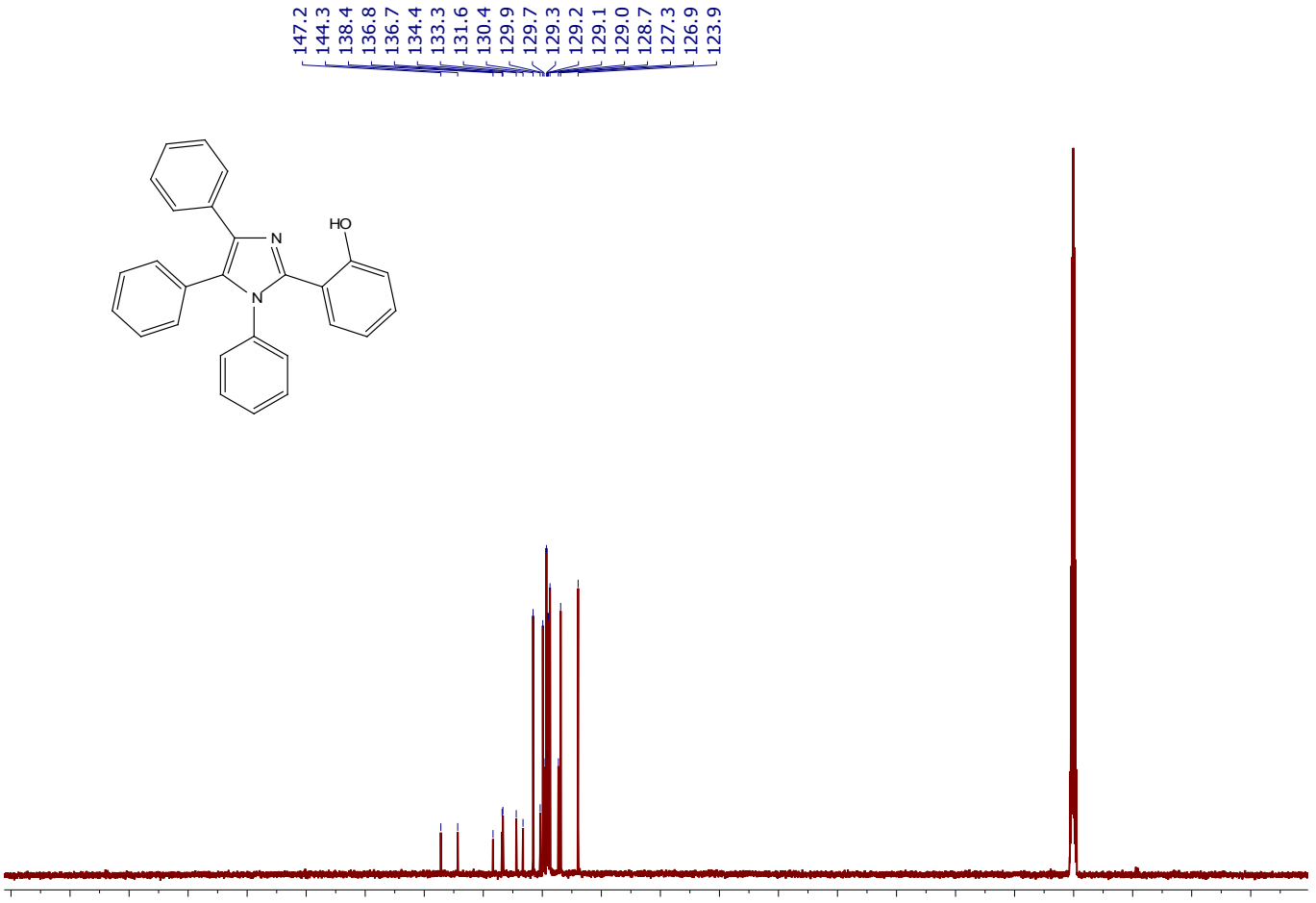

^{1}H, ^{13}C NMR spectrum of 2-(3-Hydroxyphenyl)-1,4,5-triphenyl-1*H*-imidazole (IMI-03)

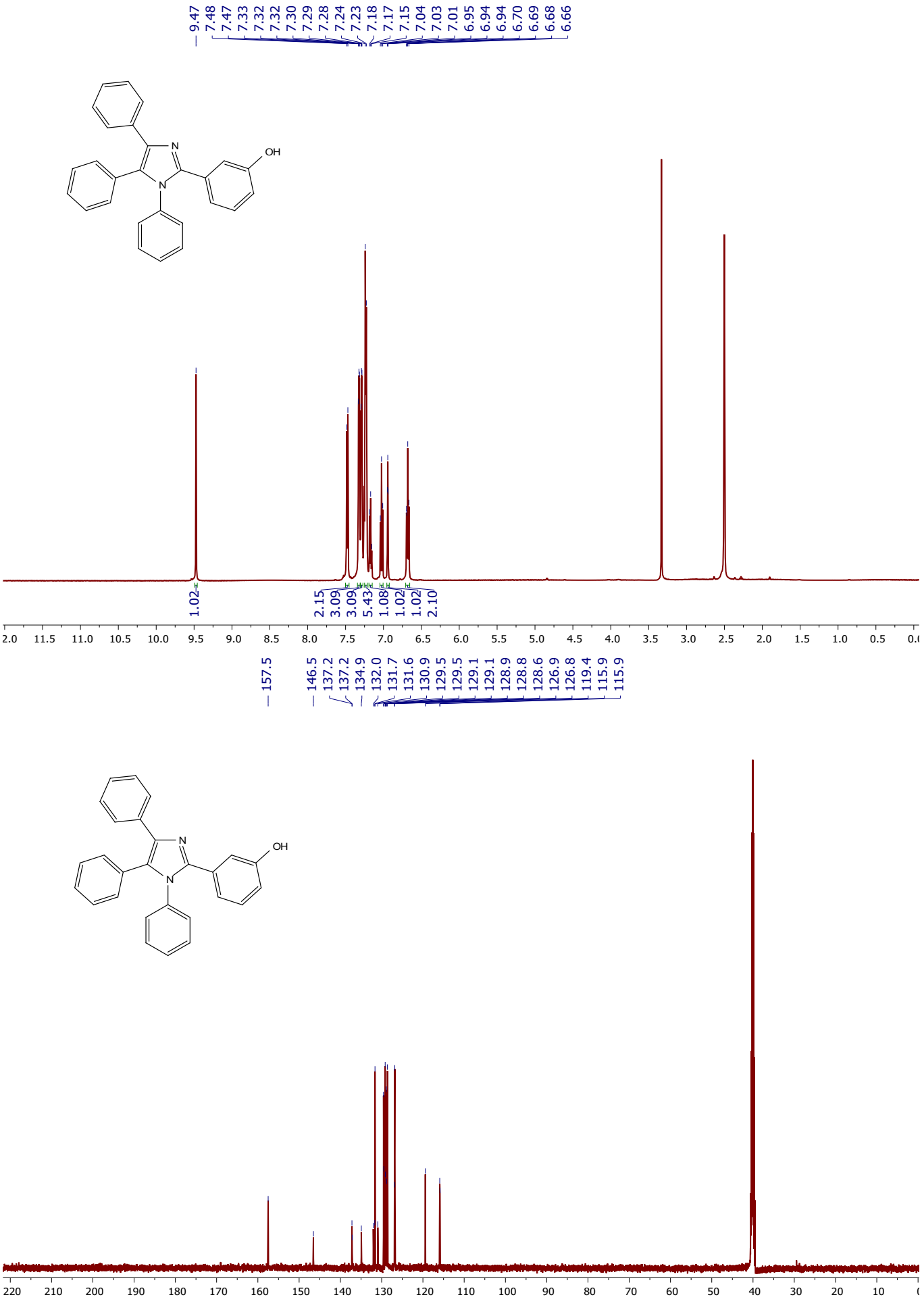

^{1}H, ^{13}C NMR spectrum of 2-(4-Hydroxy-3-methoxyphenyl)-1,4,5-triphenyl-1*H*-imidazole (IMI-04)

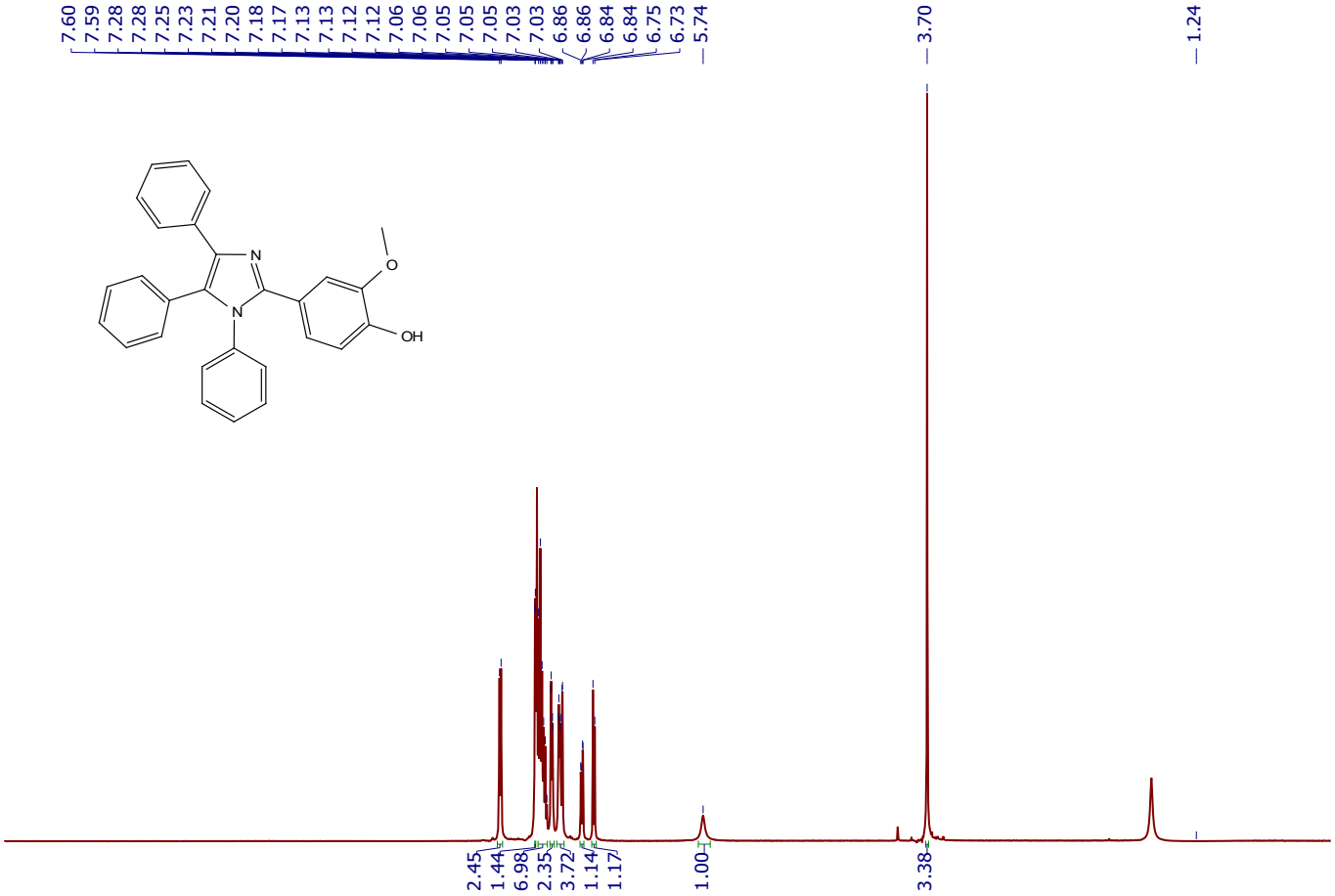

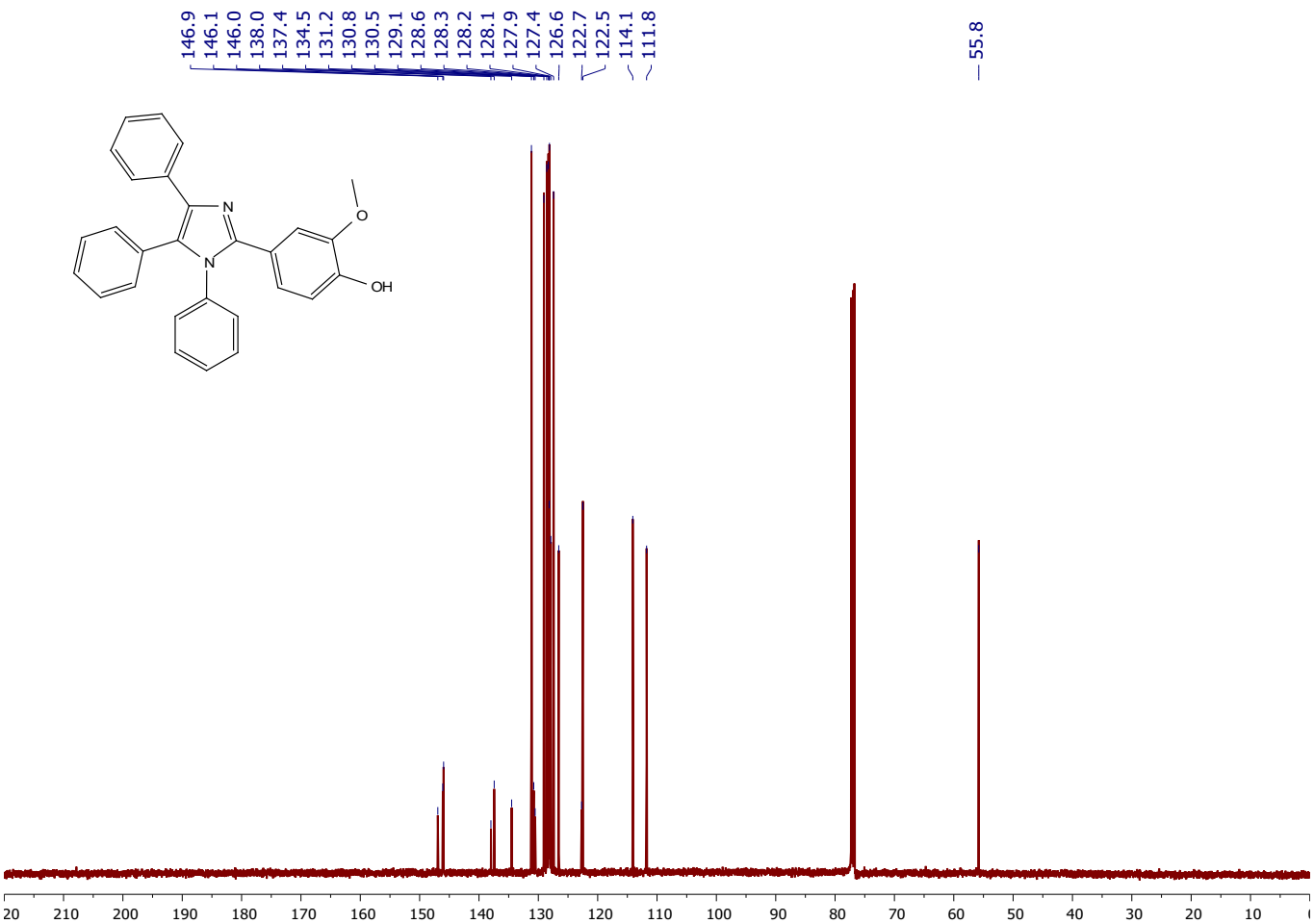

^{1}H, ^{13}C NMR spectrum of 2-(4-Nitrophenyl)-1,4,5-triphenyl-1*H*-imidazole (IMI-05)

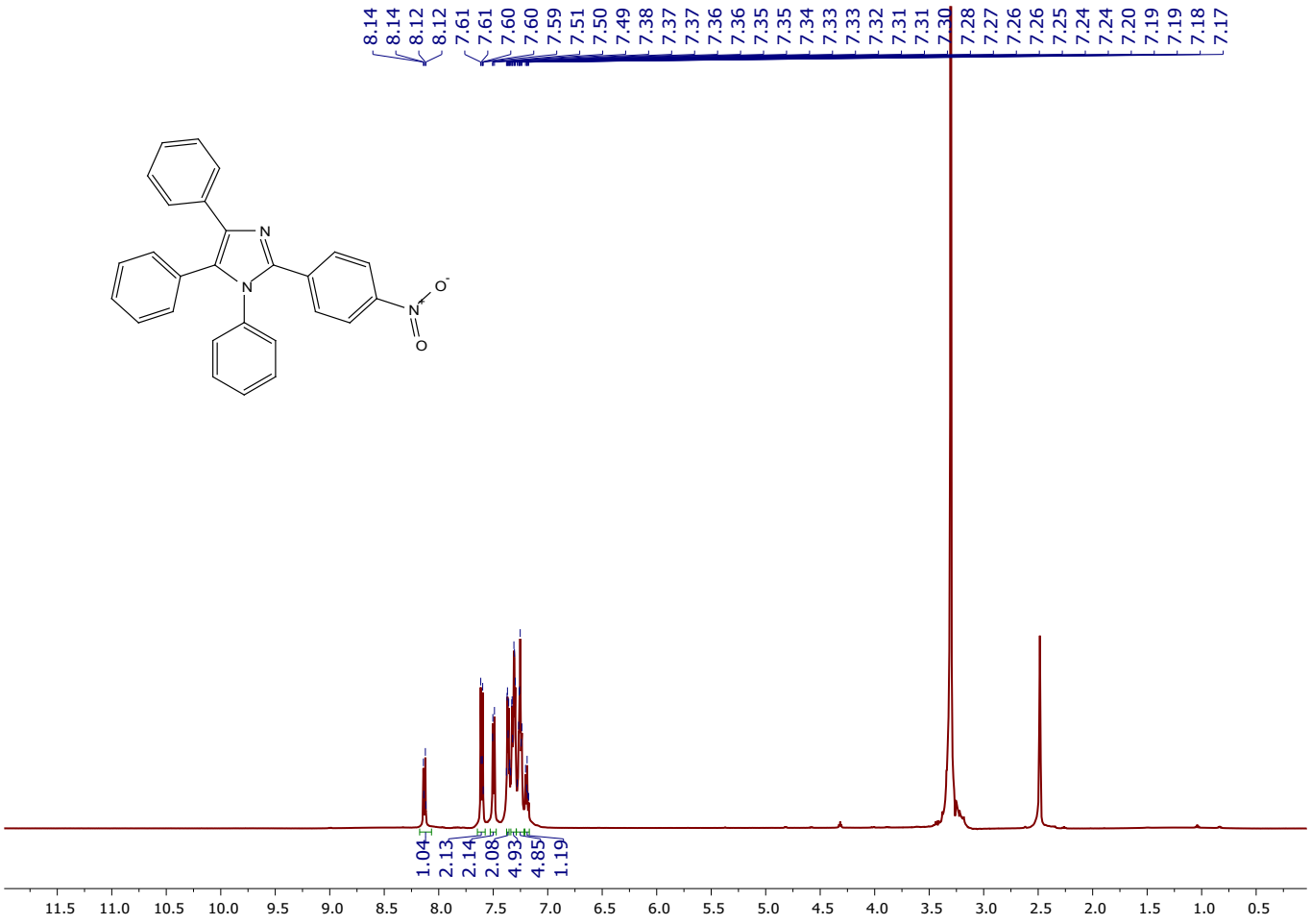

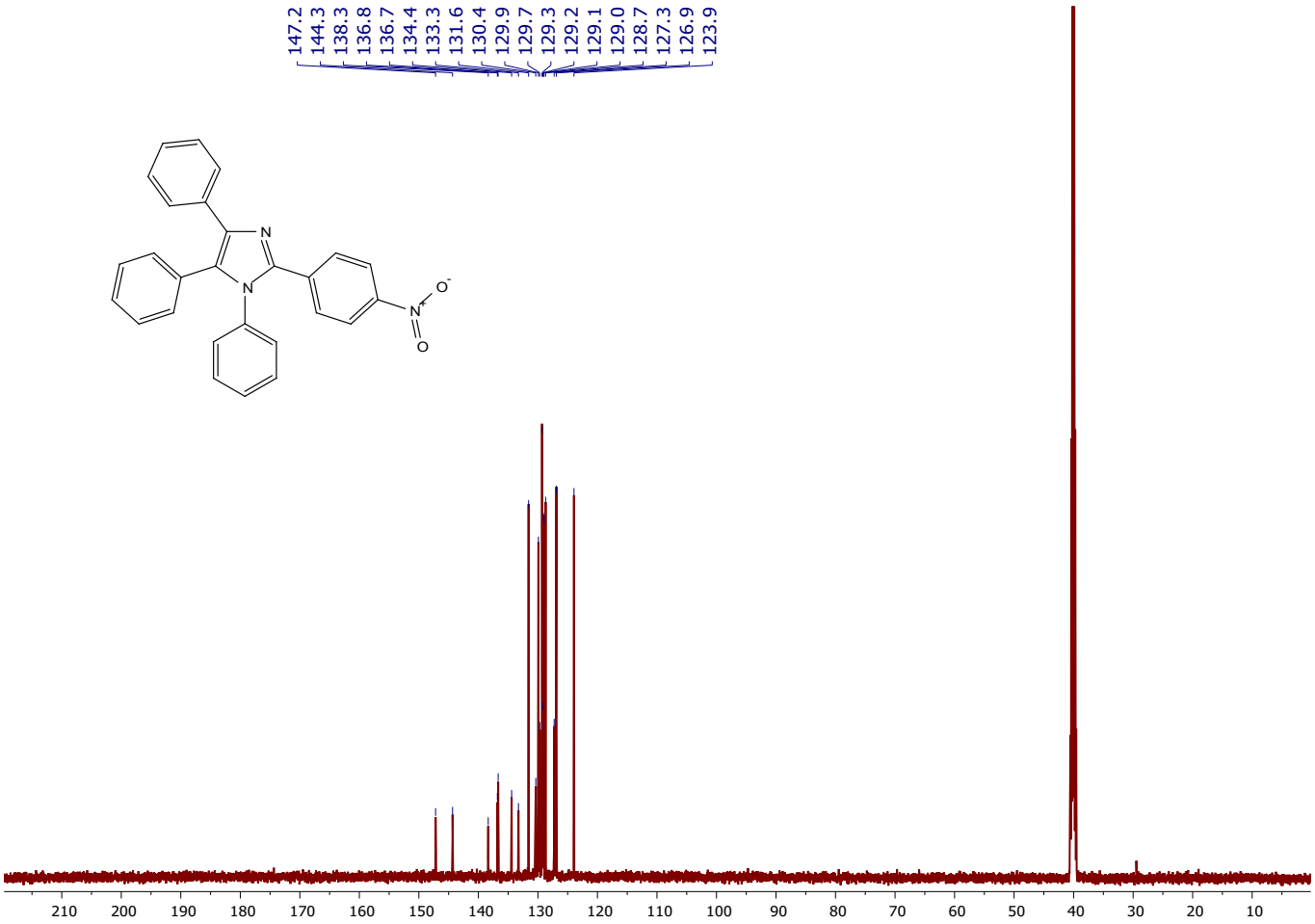

^{1}H, ^{13}C NMR spectrum of 2-(4-Hydroxyphenyl)-1,4,5-triphenyl-1*H*-imidazole (IMI-06)

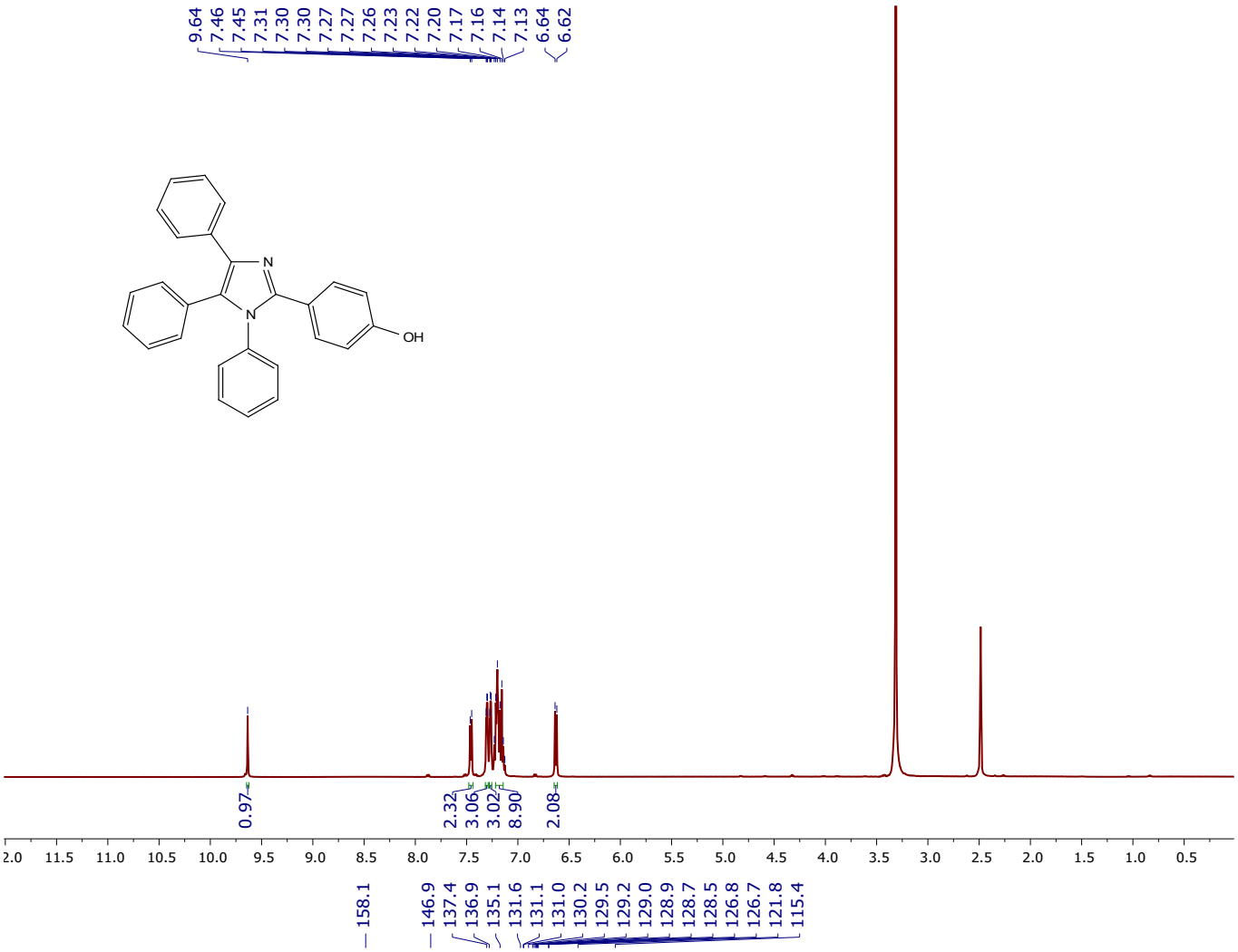

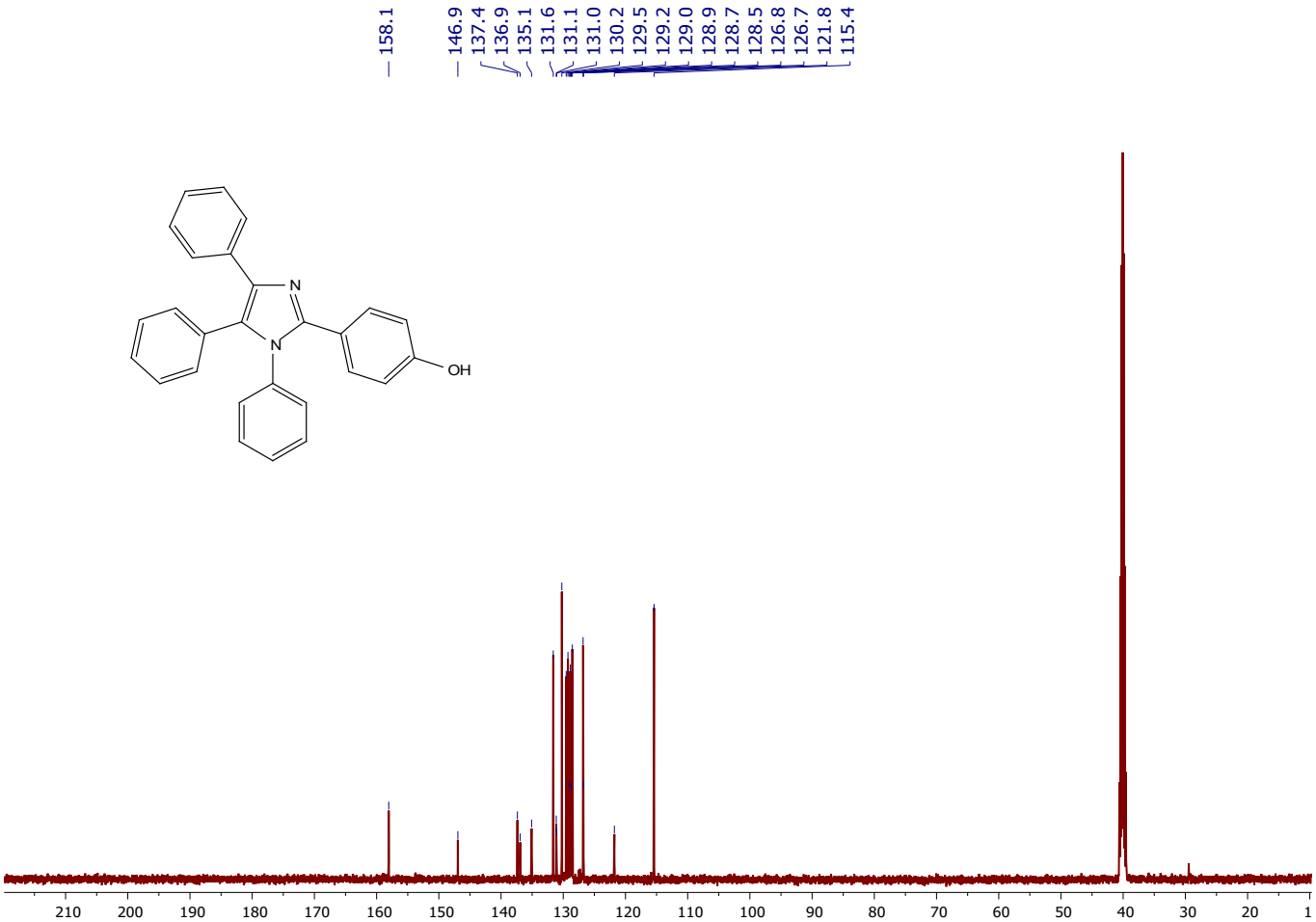

^{1}H, ^{13}C NMR spectrum of 2-(4-Bromophenyl)-1,4,5-triphenyl-1*H*-imidazole (IMI-07)

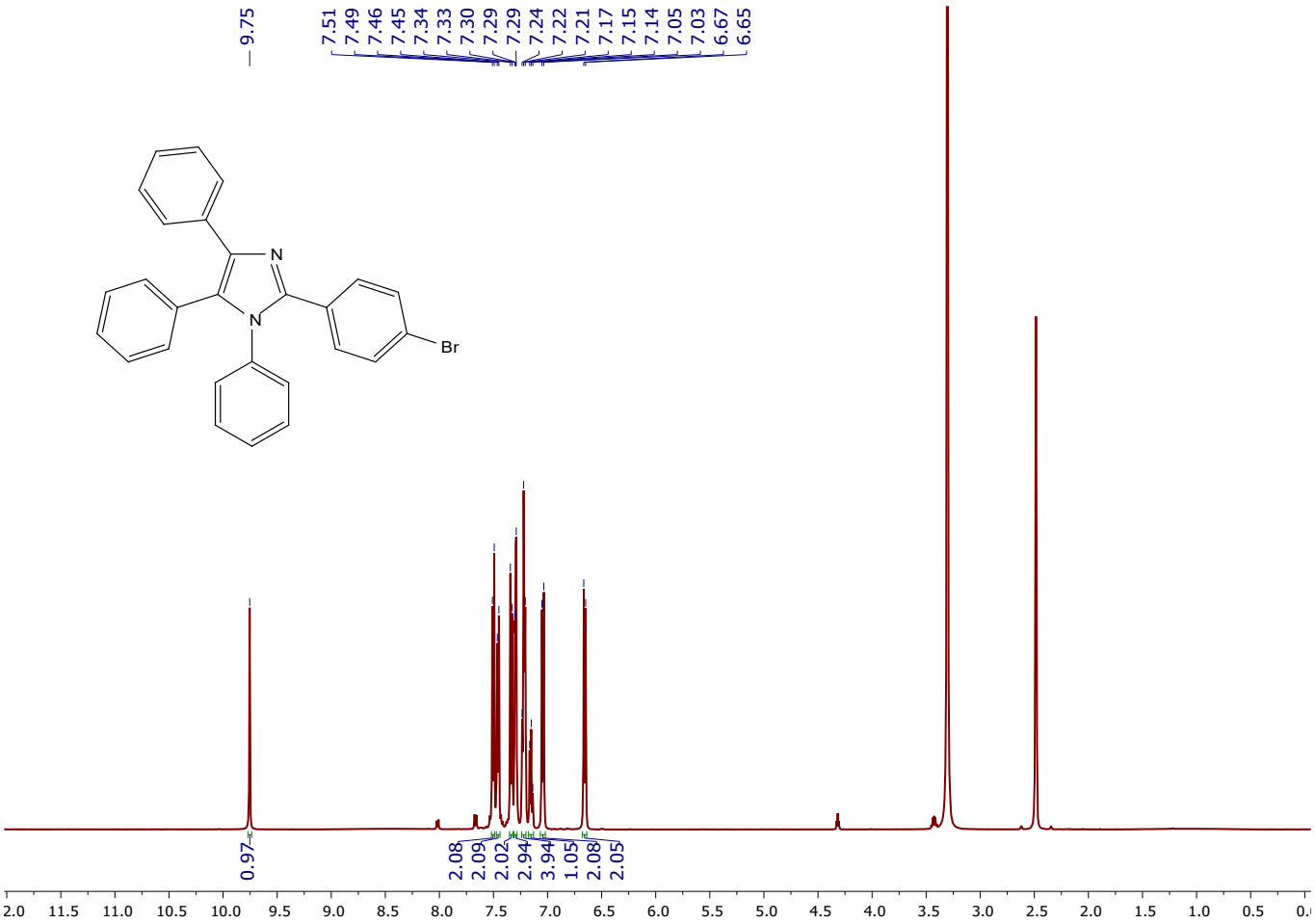

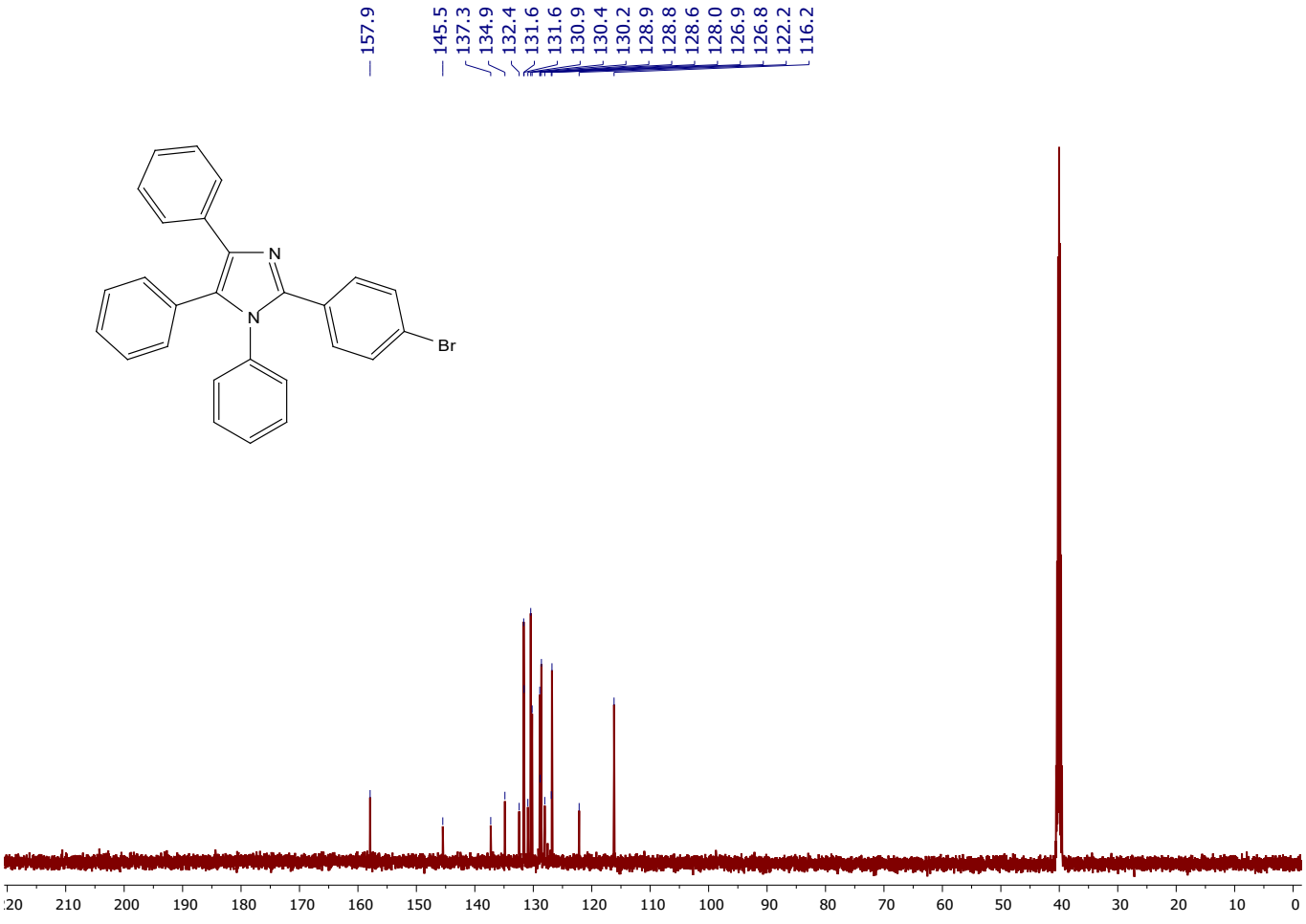

^{1}H, ^{13}C NMR spectrum of 2-(4-*N*,*N*-dimethylaminophenyl)-1,4,5-triphenyl-1*H*-imidazole (IMI-08)

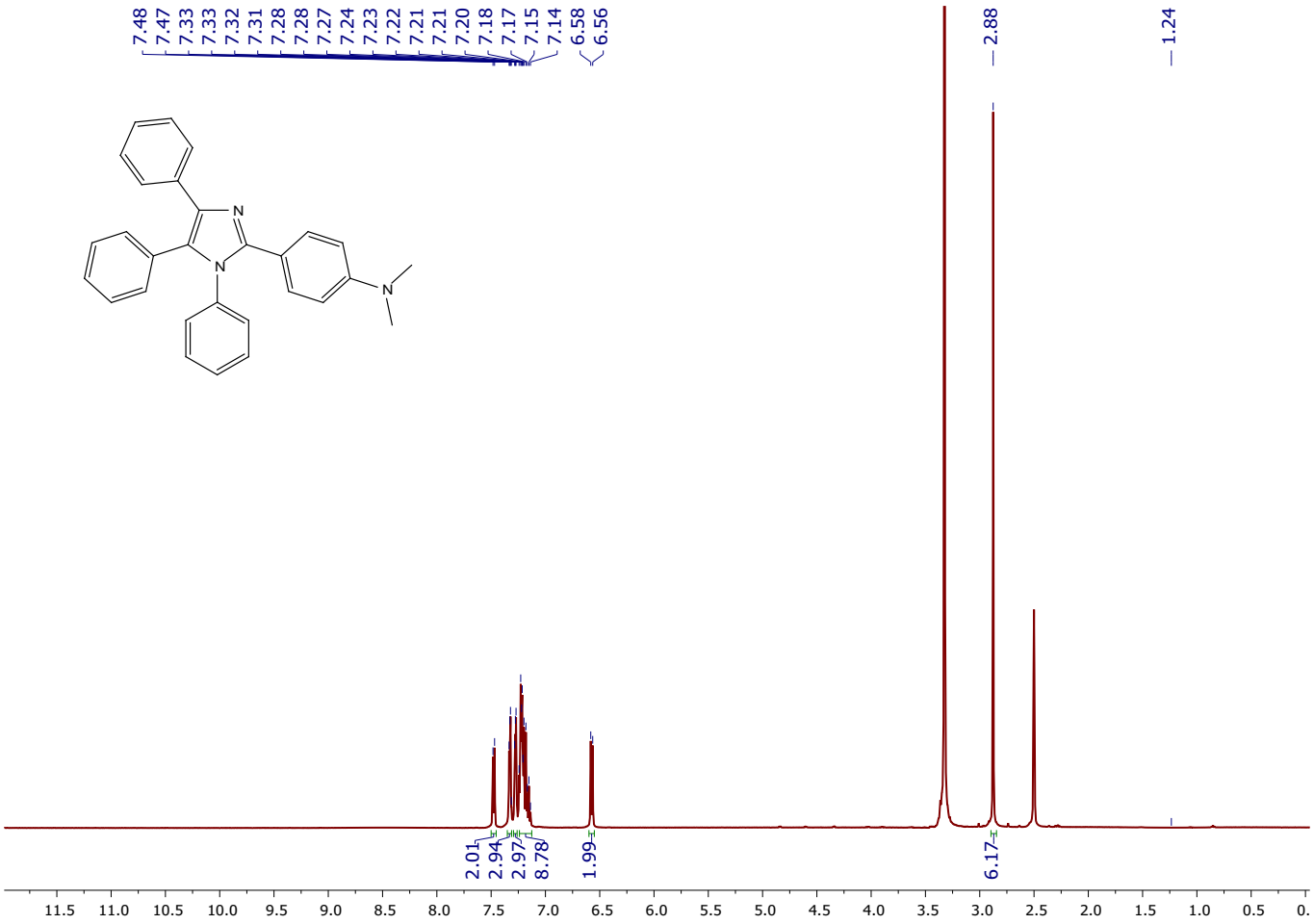

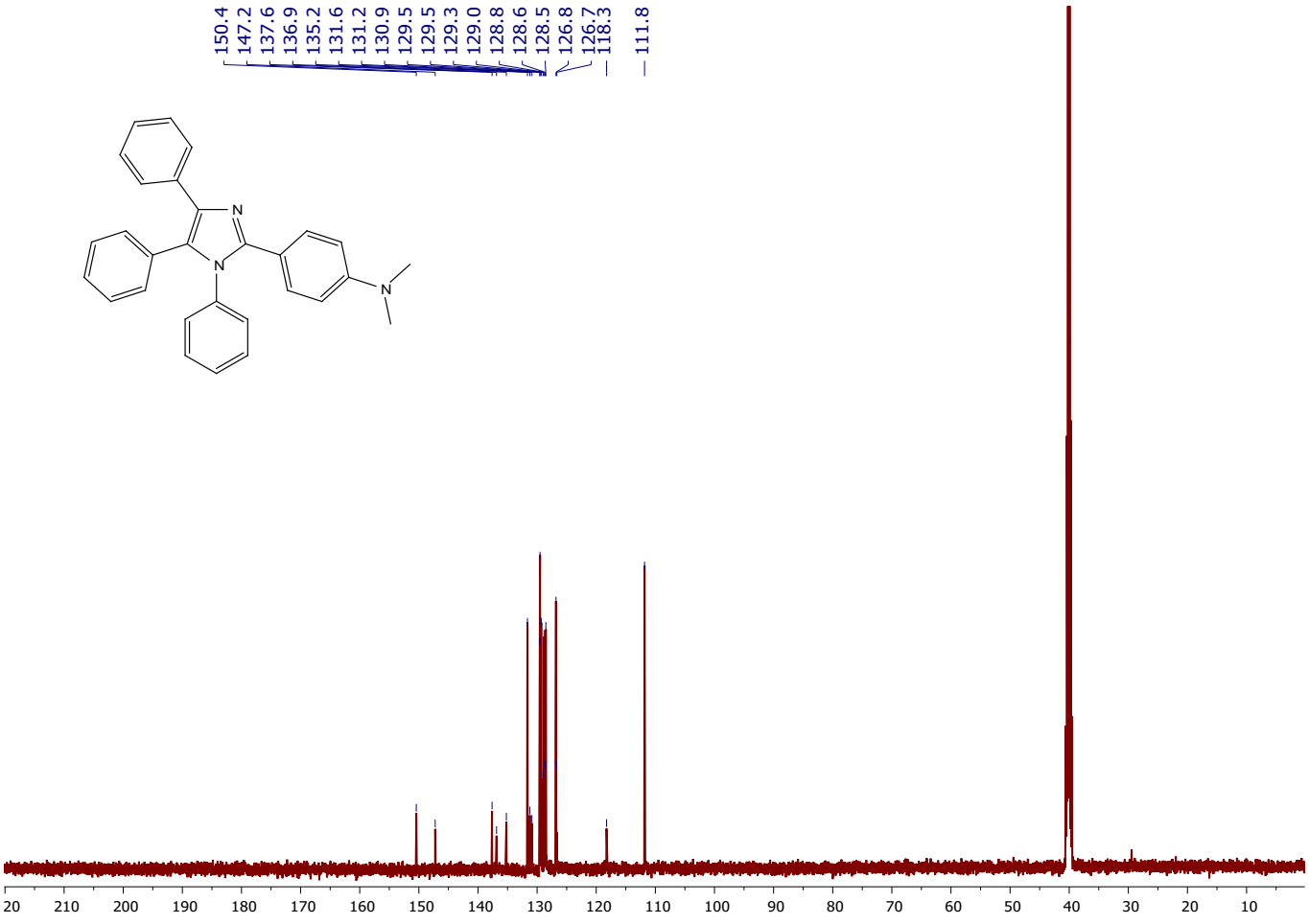

^{1}H, ^{13}C NMR spectrum of 2-(4-Methylphenyl)-1,4,5-triphenyl-1*H*-imidazole (IMI-09)

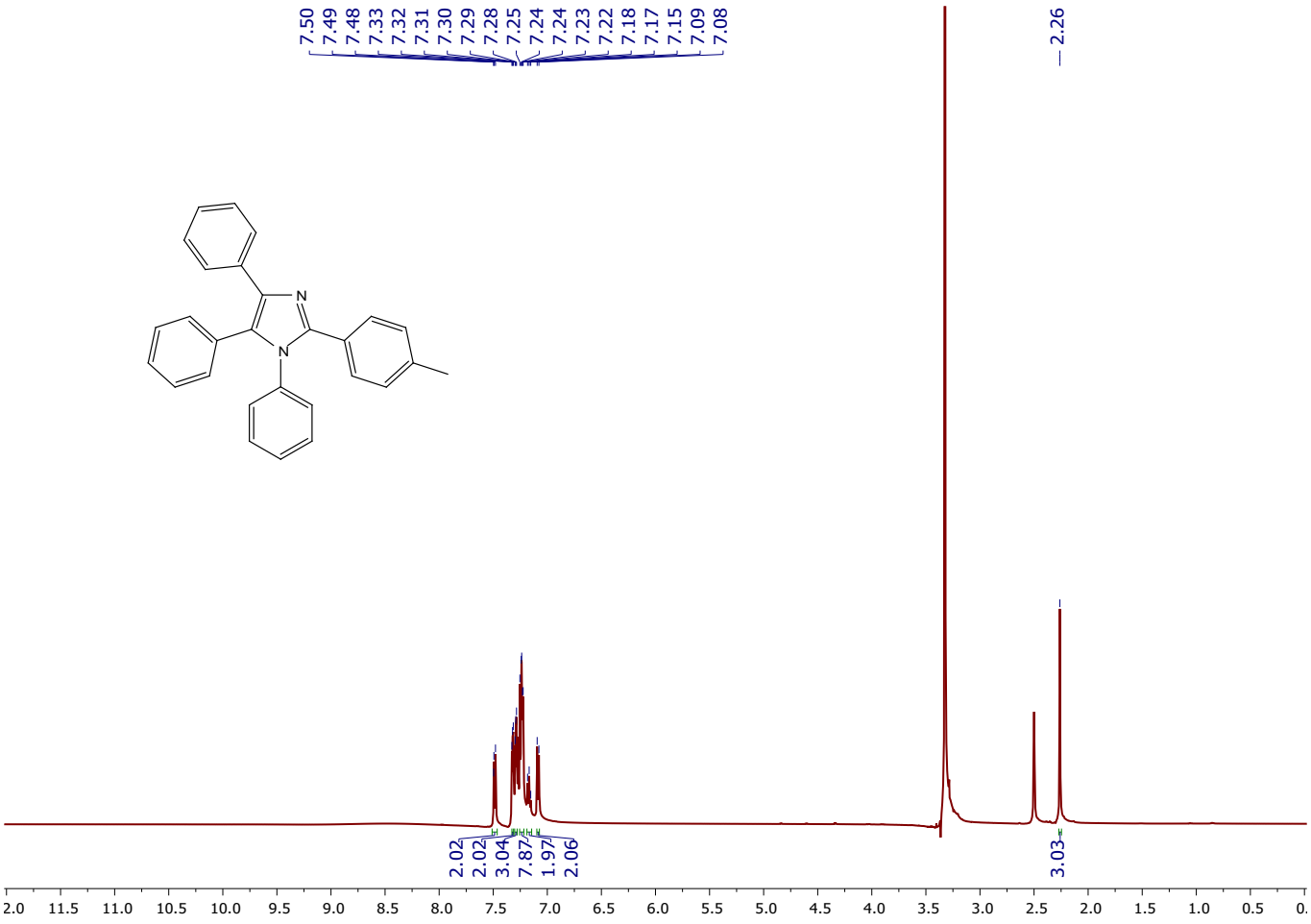

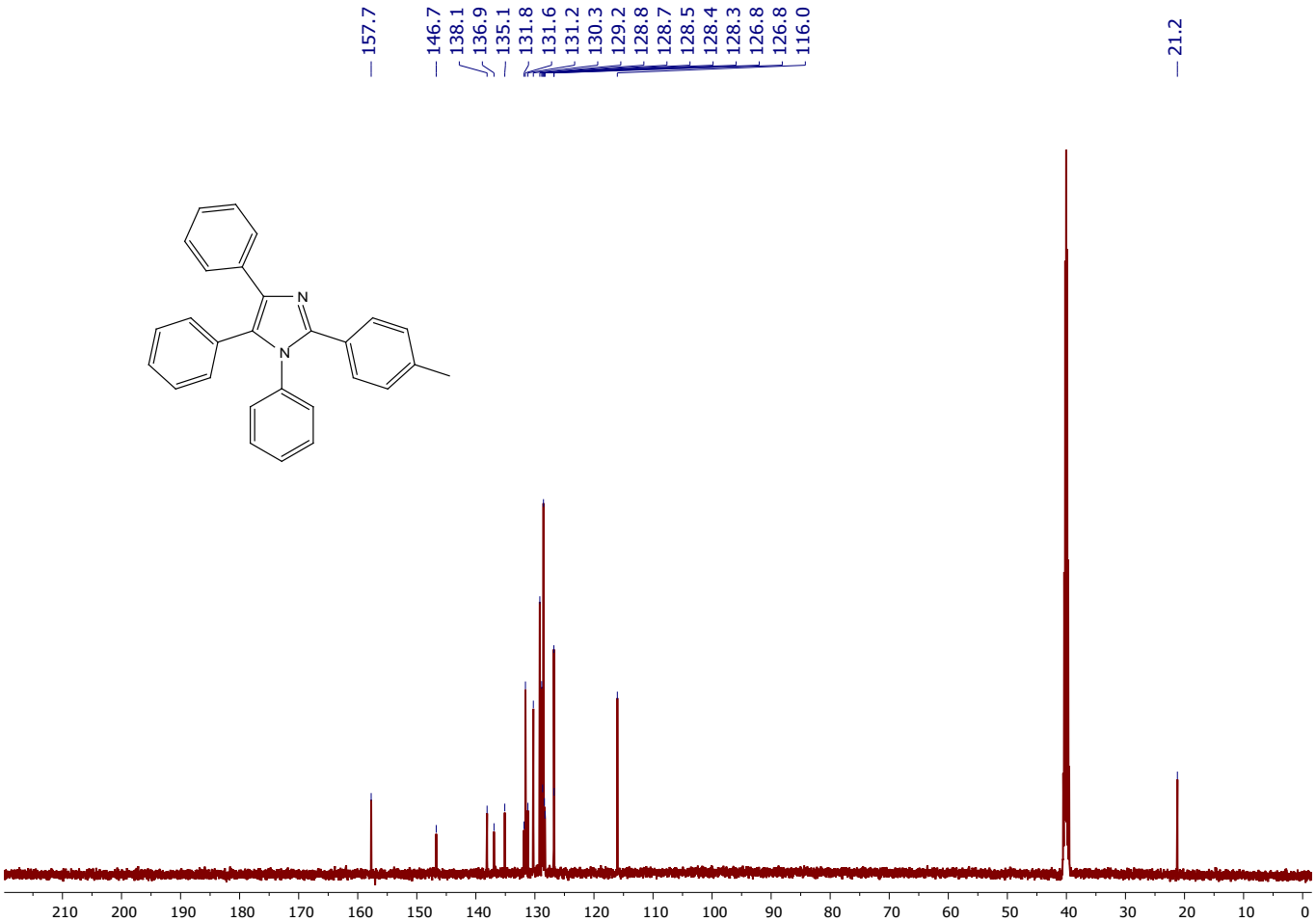

^{1}H, ^{13}C NMR spectrum of 2-Cyclohexyl-1,4,5-triphenyl-1*H*-imidazole (IMI-10)

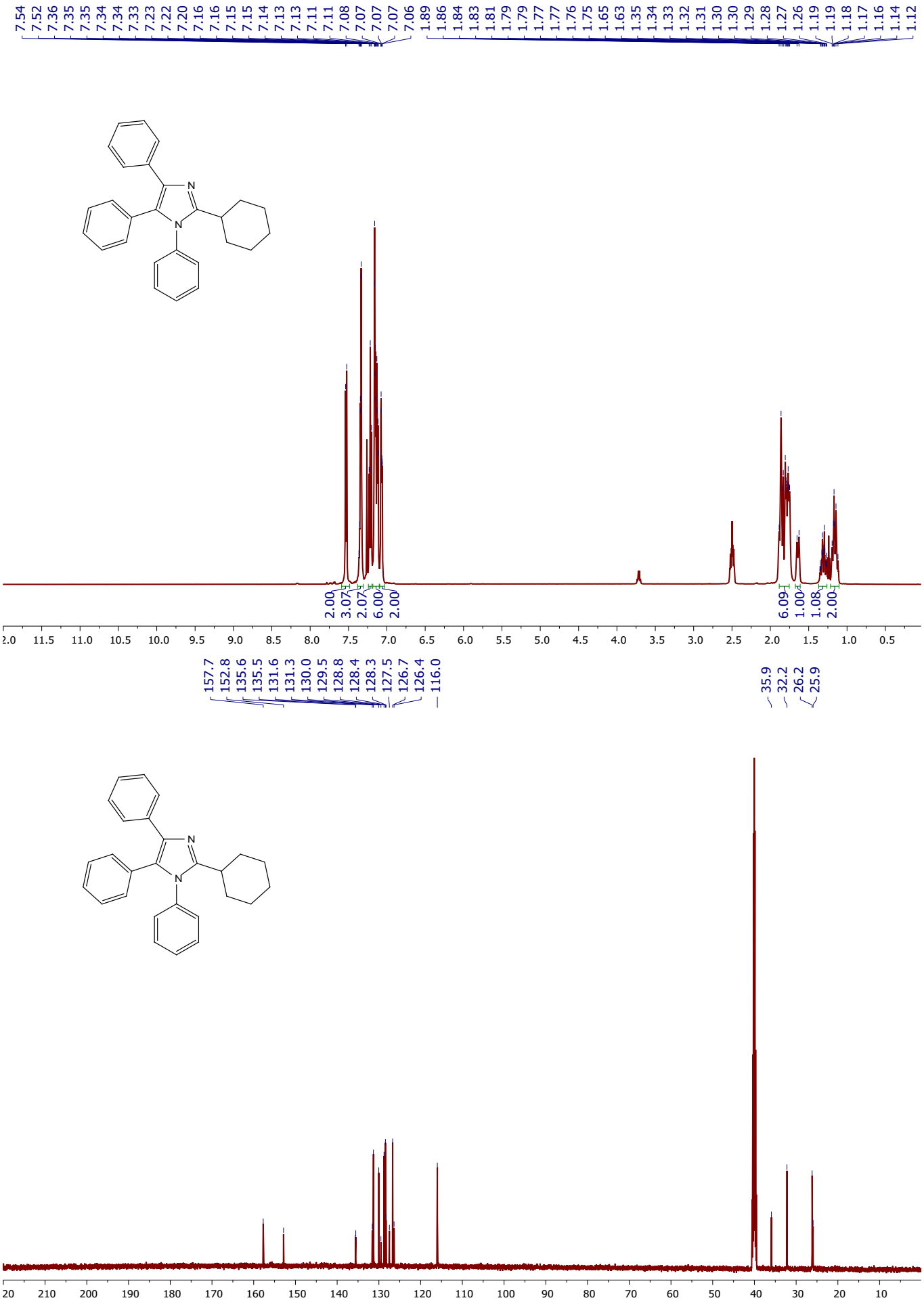

^{1}H, ^{13}C NMR spectrum of 2-(Furan-2-yl)-1,4,5-triphenyl-1*H*-imidazole (IMI-11)

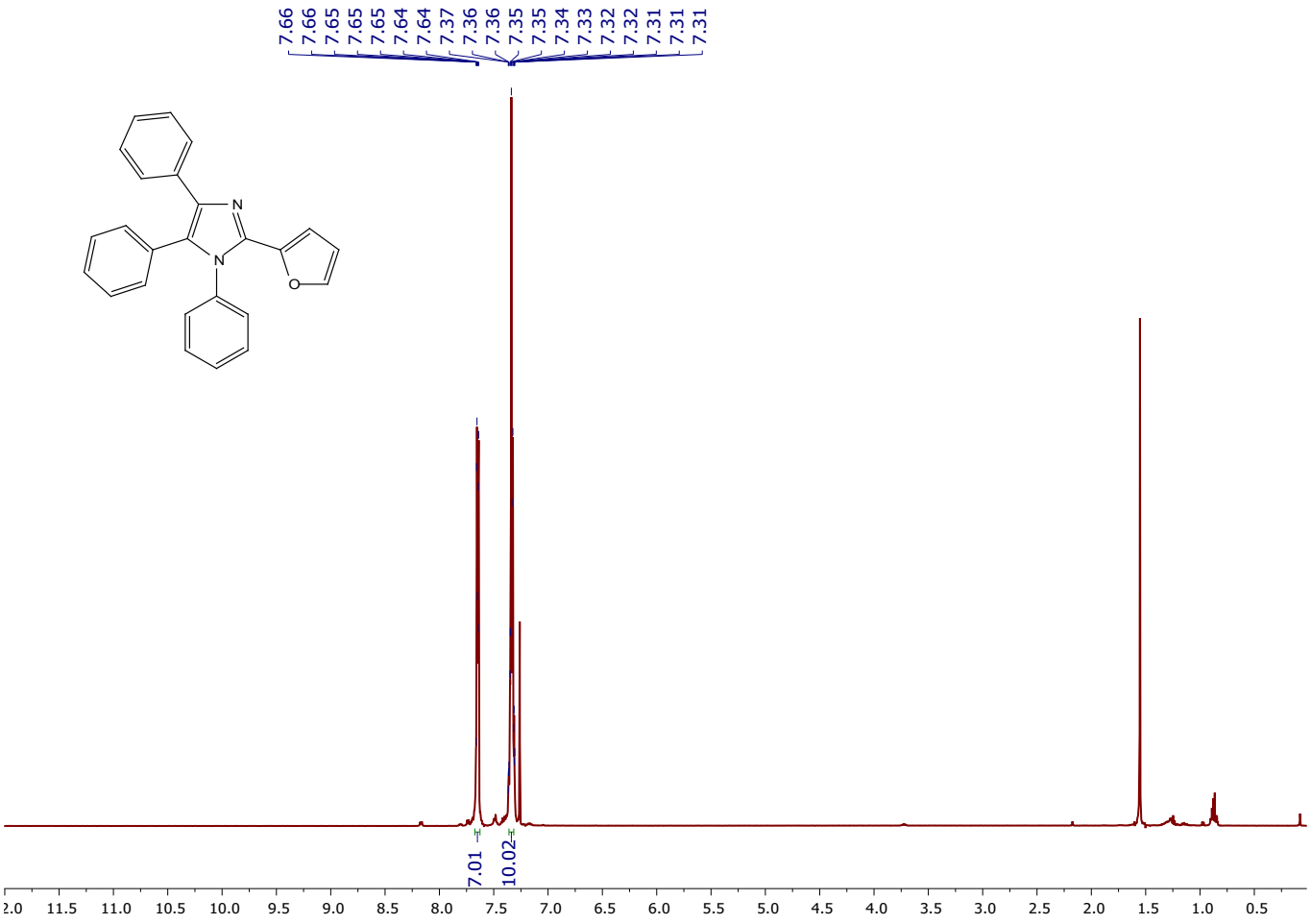

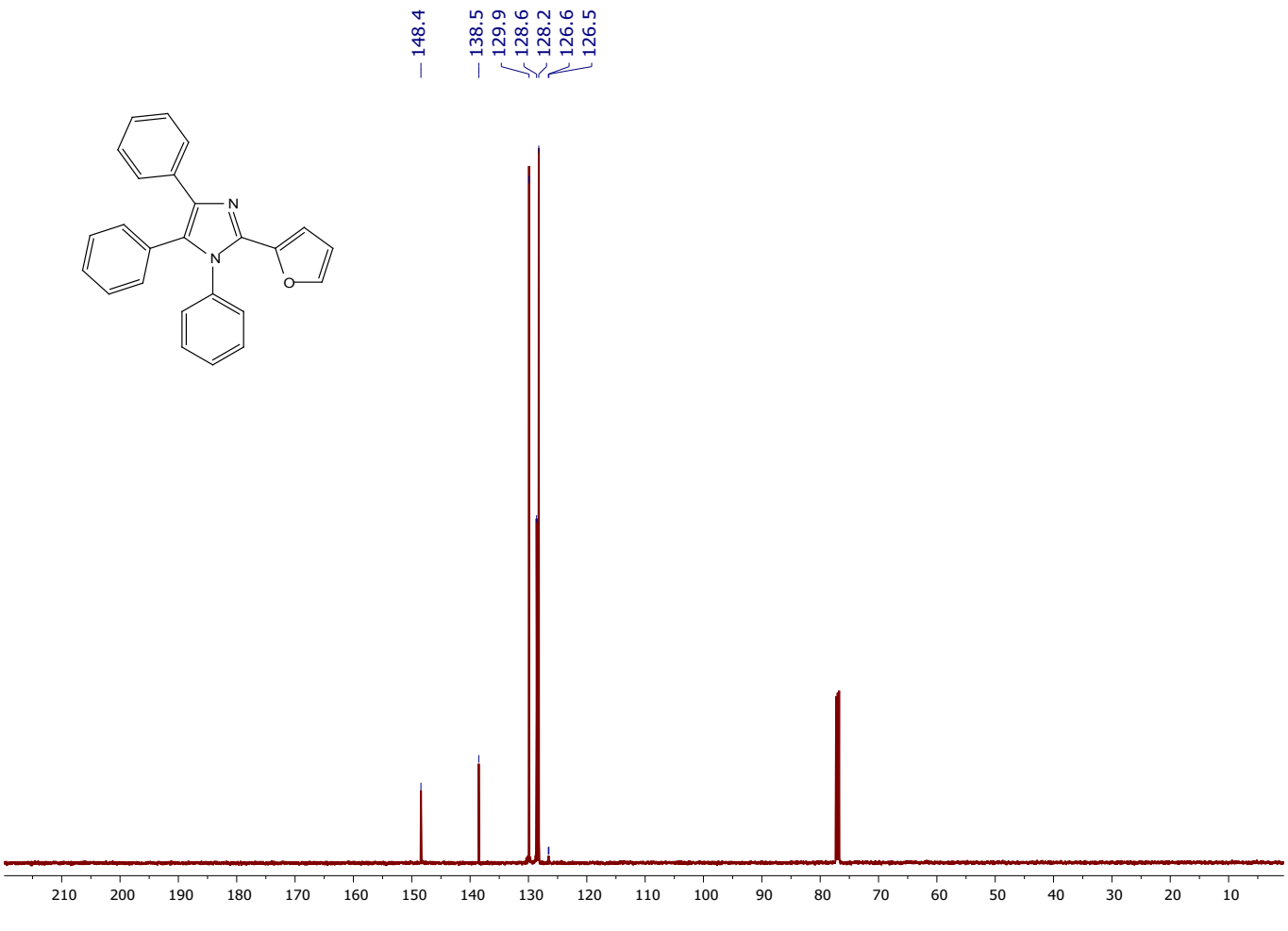

^{1}H, ^{13}C NMR spectrum of 1-(4-Hydroxyphenyl)-2,4,5-triphenyl-1*H*-imidazole (IMI-12)

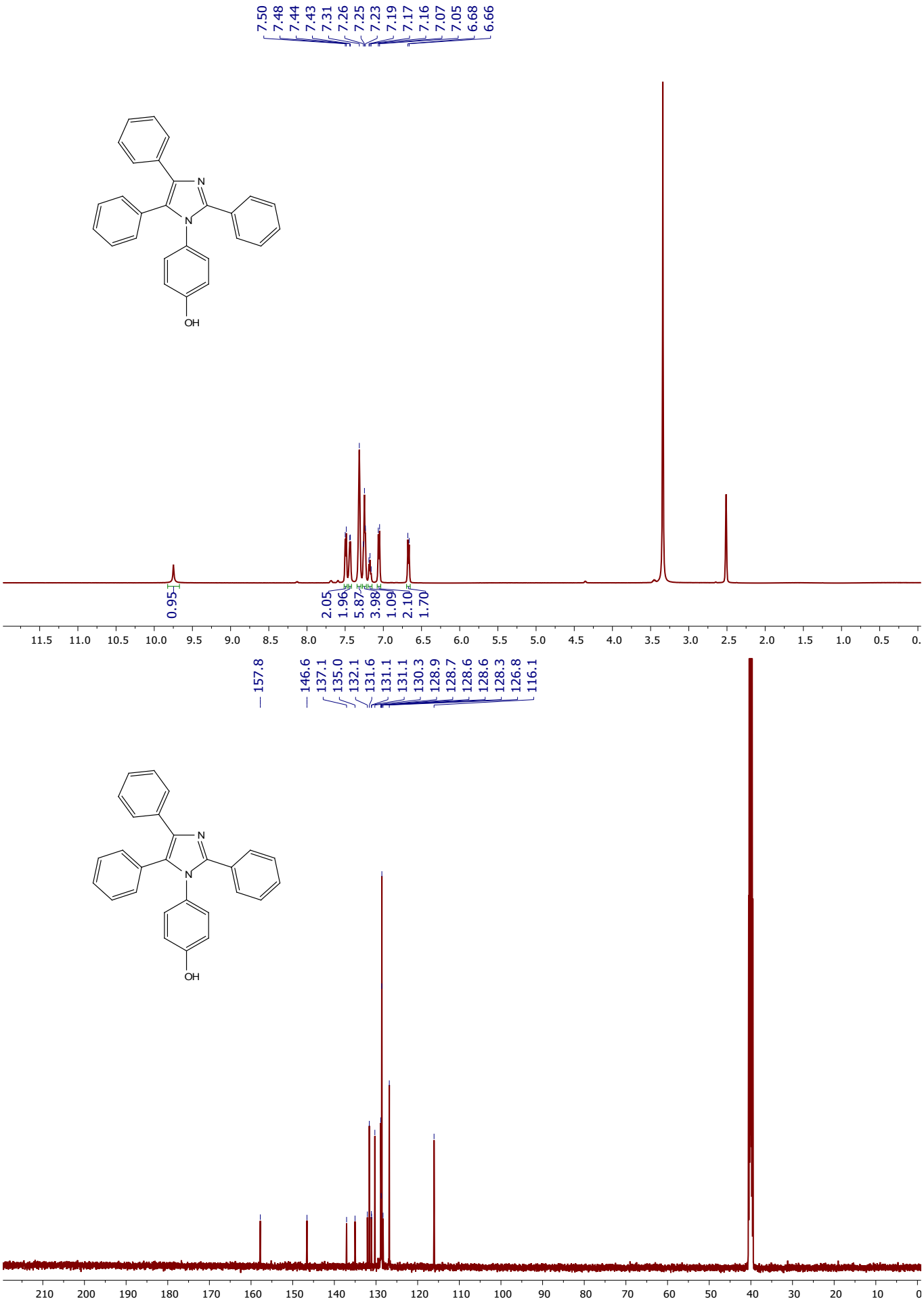

^{1}H, ^{13}C NMR spectrum of 1-(4-Hydroxyphenyl)-2-(4-hydroxyl-3-methoxyphenyl)-4,5-diphenyl-1*H*-imidazole (IMI-13)

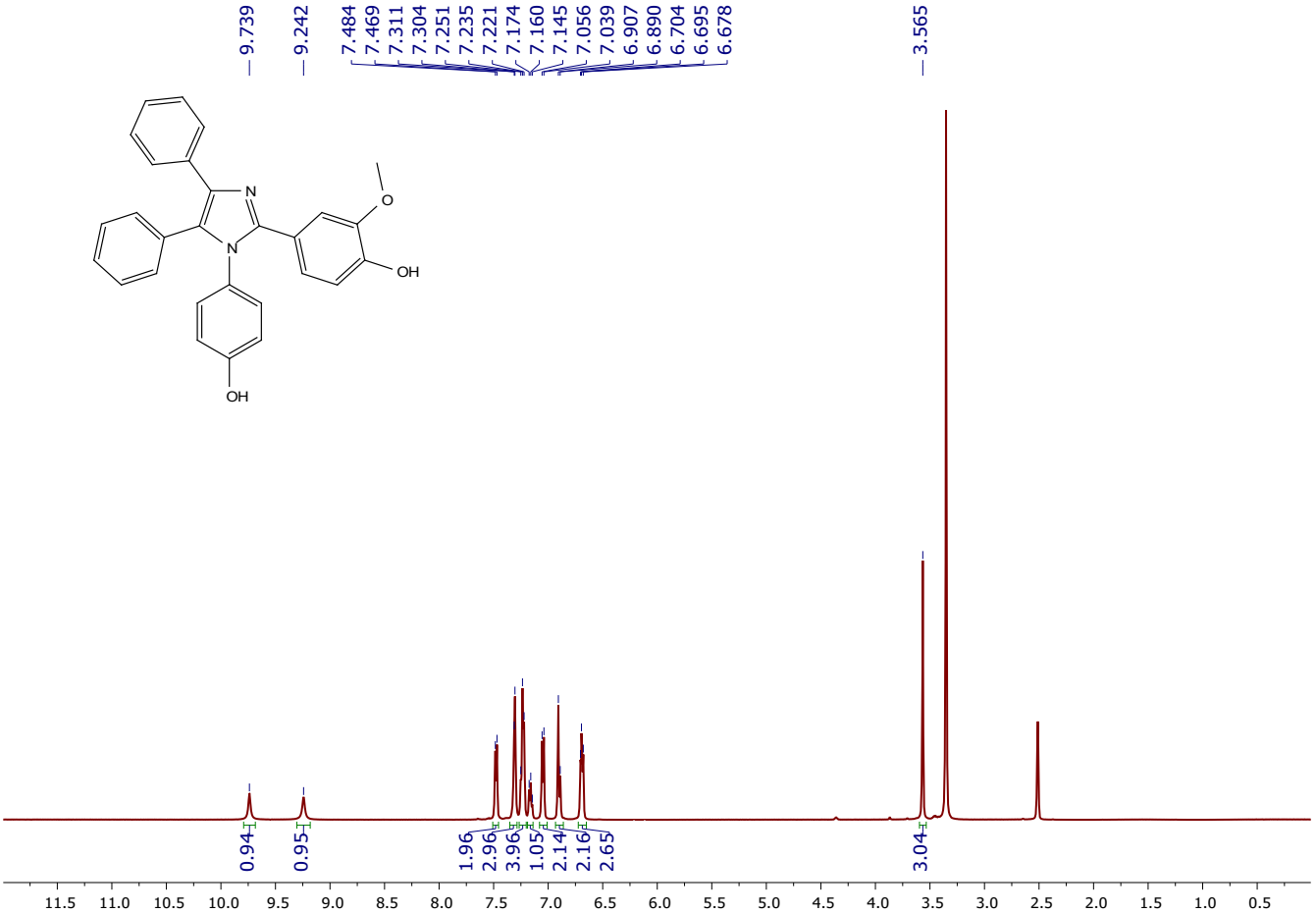

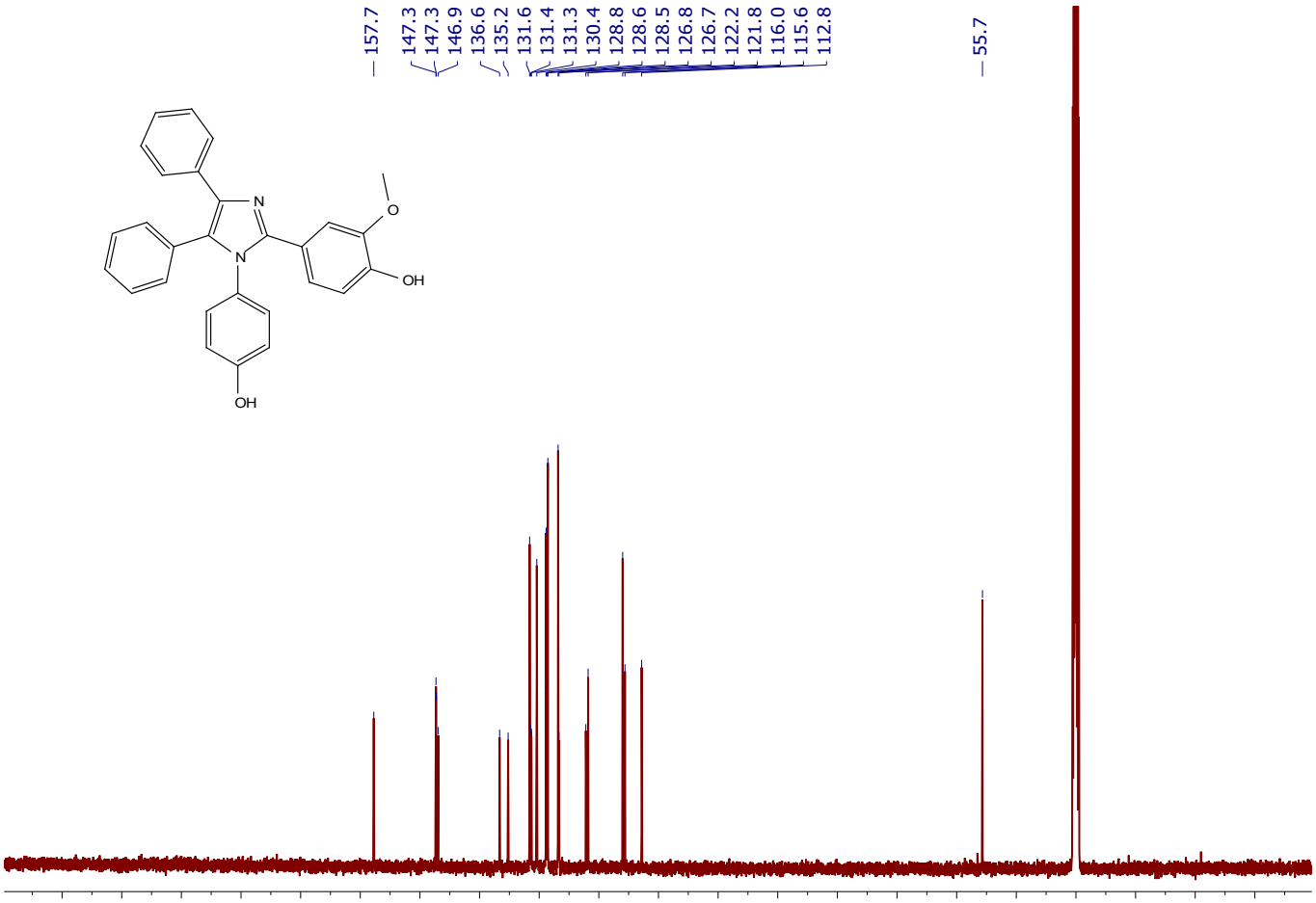

^{1}H, ^{13}C NMR spectrum of 1-(4-Hydroxyphenyl)-2-(4-nitrophenyl)-4,5-diphenyl-1*H*-imidazole (IMI-14)

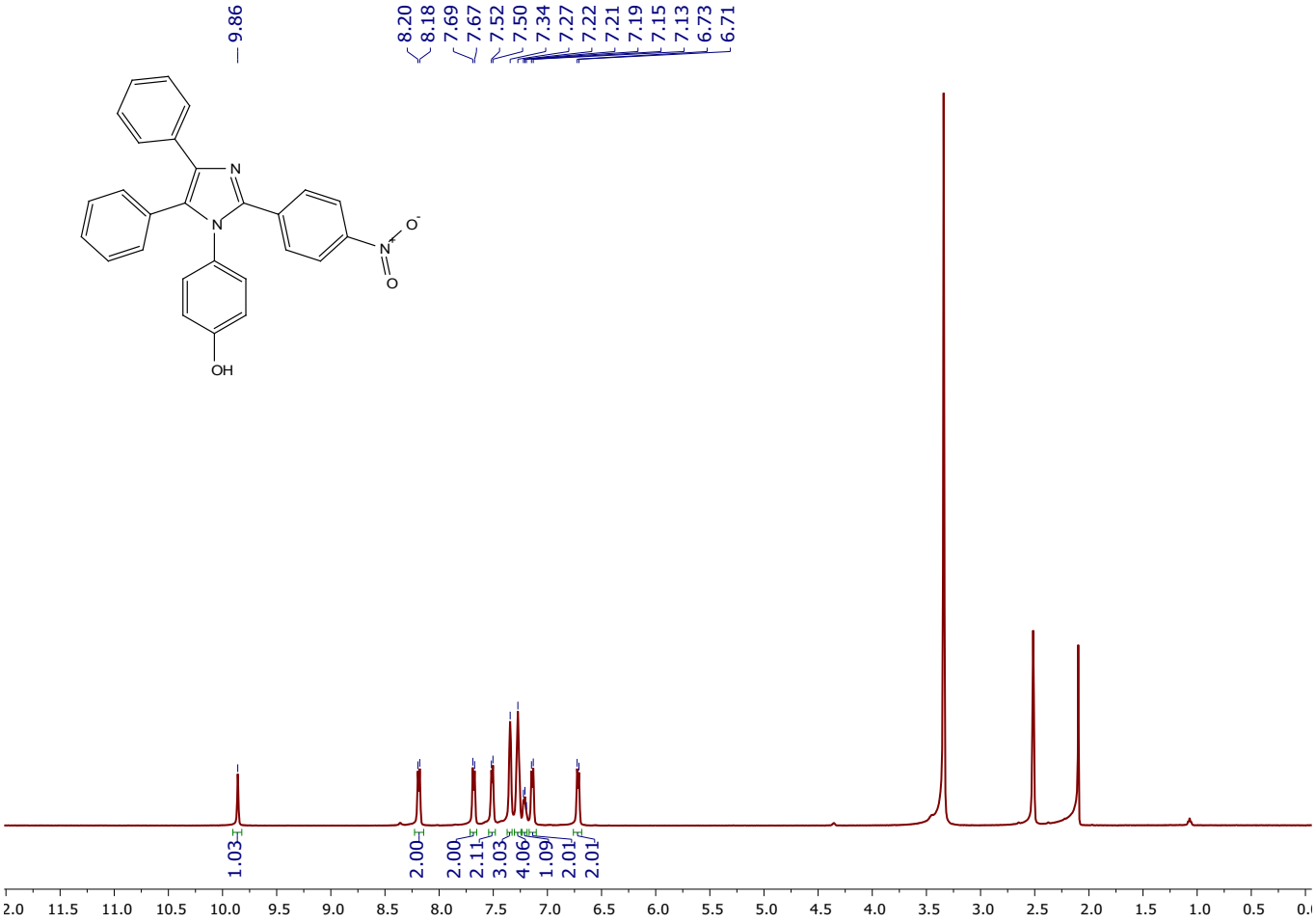

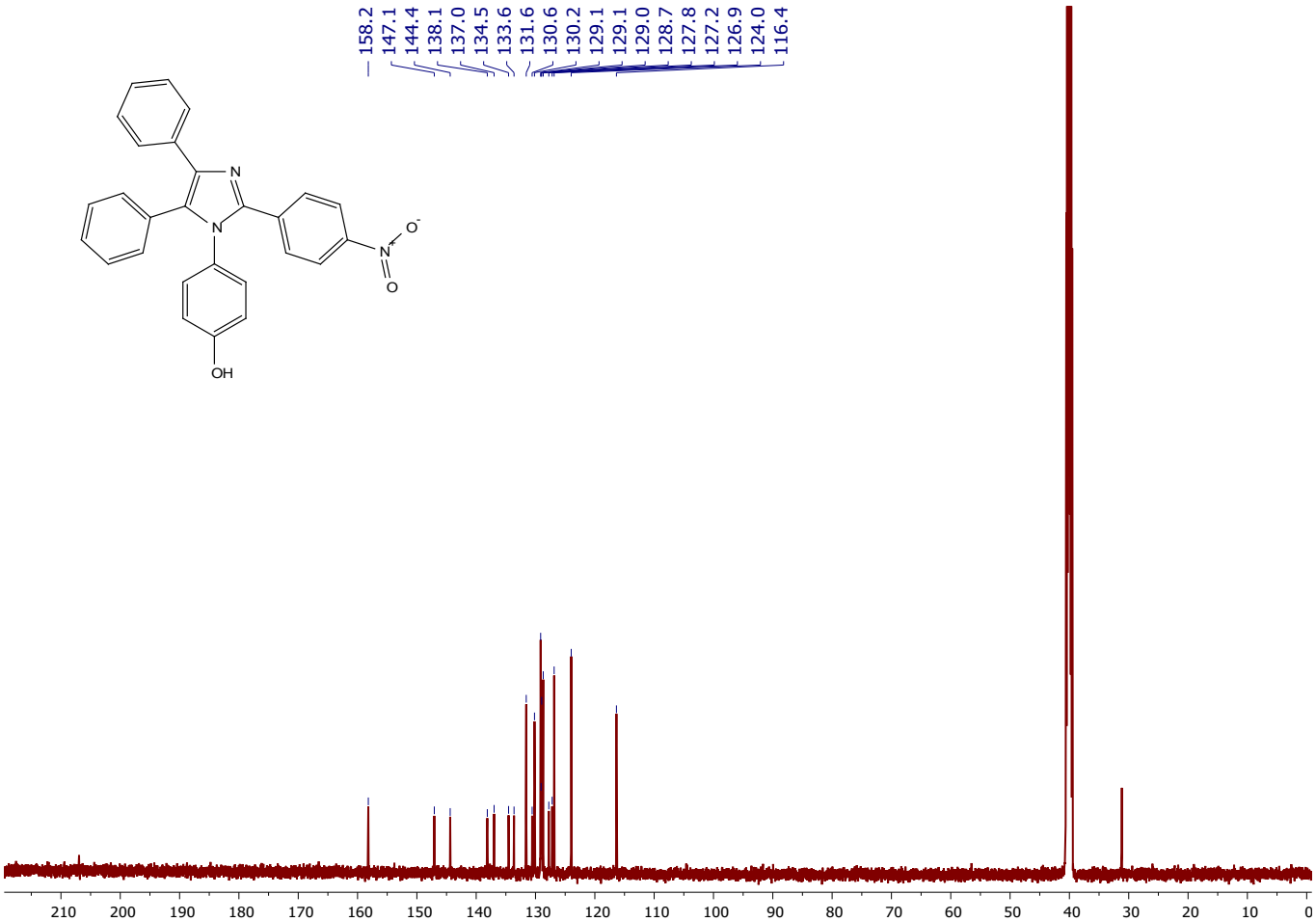

^{1}H, ^{13}C NMR spectrum of 1,2-(4-Hydroxyphenyl)-4,5-diphenyl-1*H*-imidazole (IMI-15)

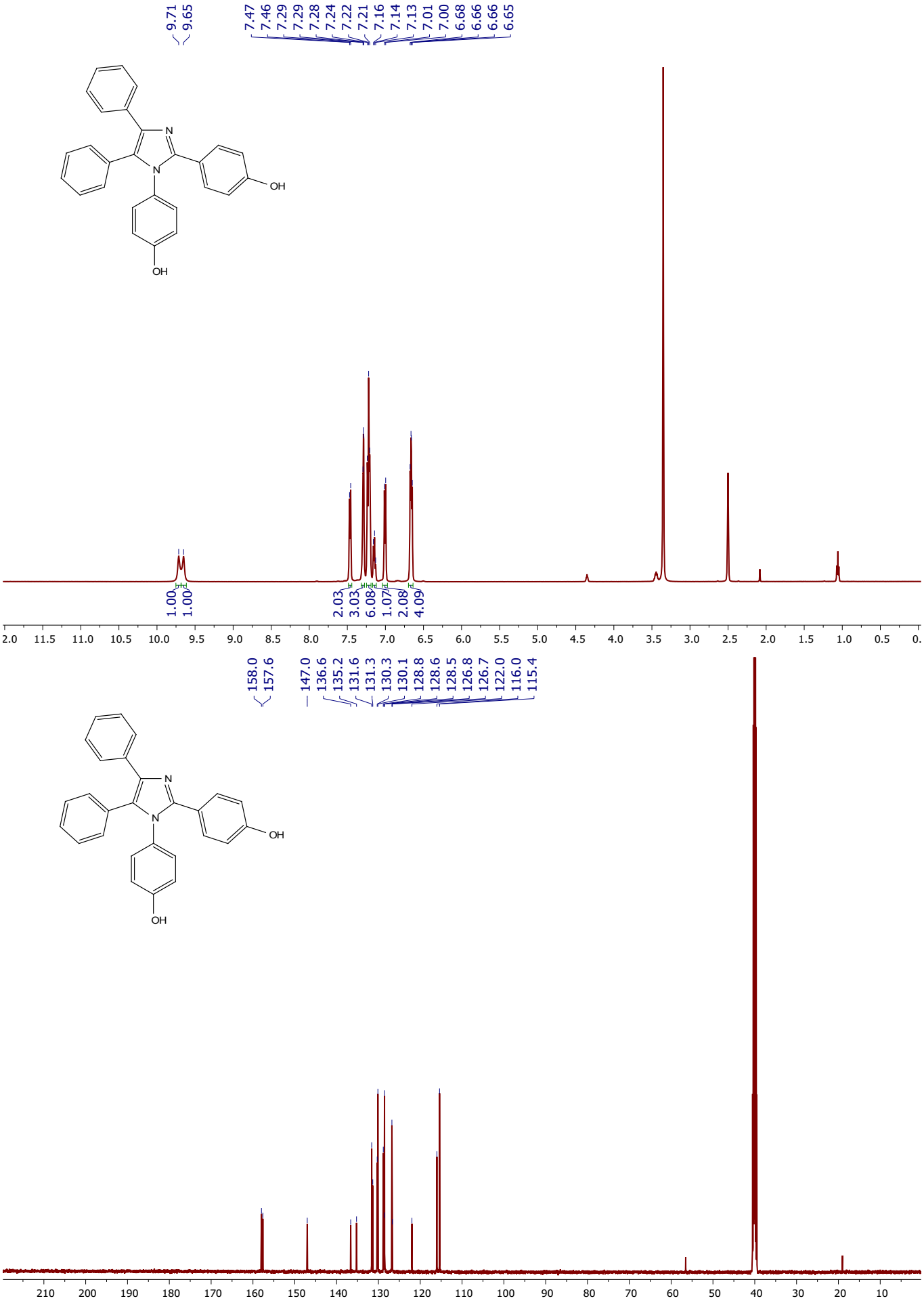

^{1}H, ^{13}C NMR spectrum of 1-(4-Hydroxyphenyl)-2-(4-methylphenyl)-4,5-diphenyl-1*H*-imidazole (IMI-16)

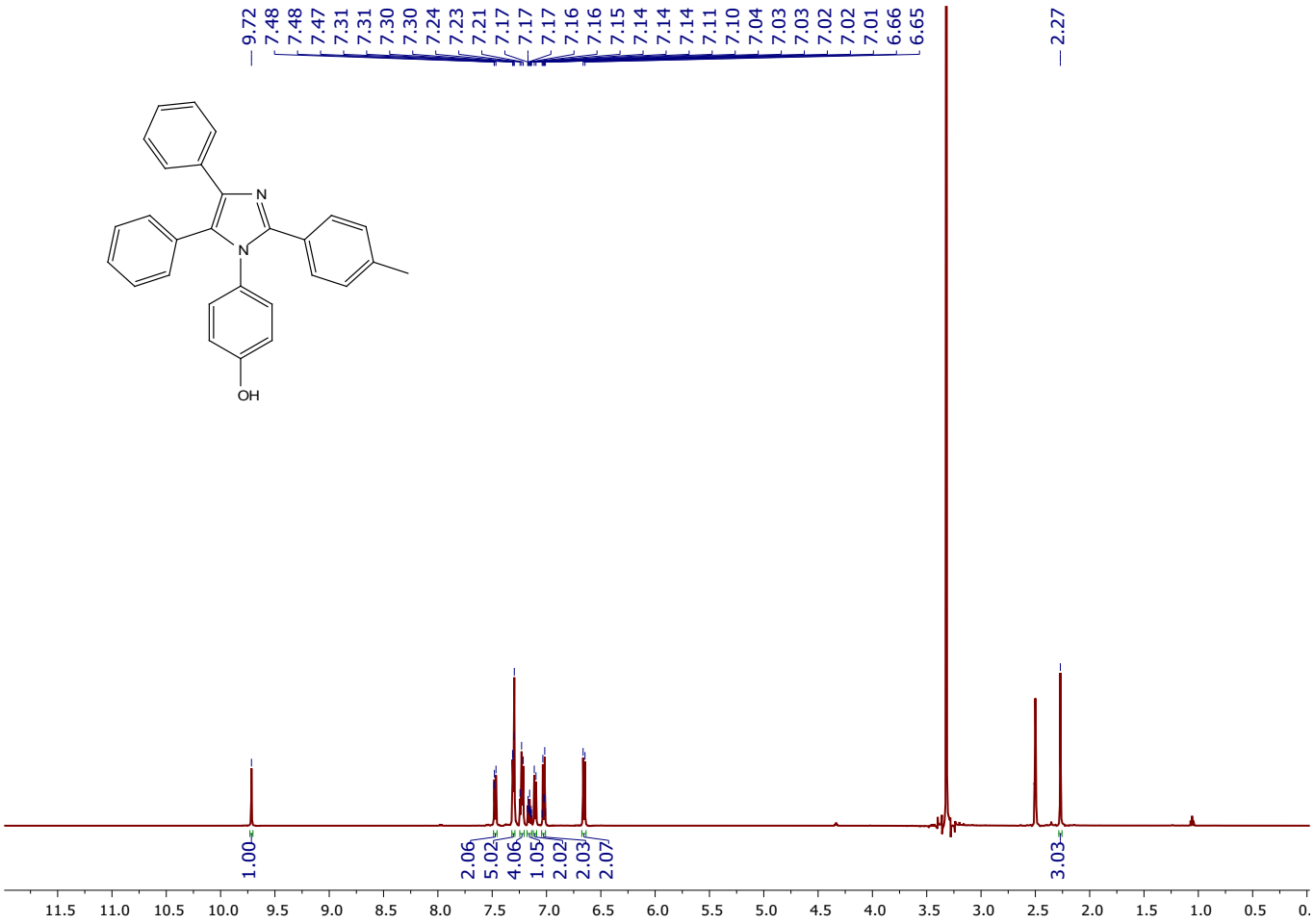

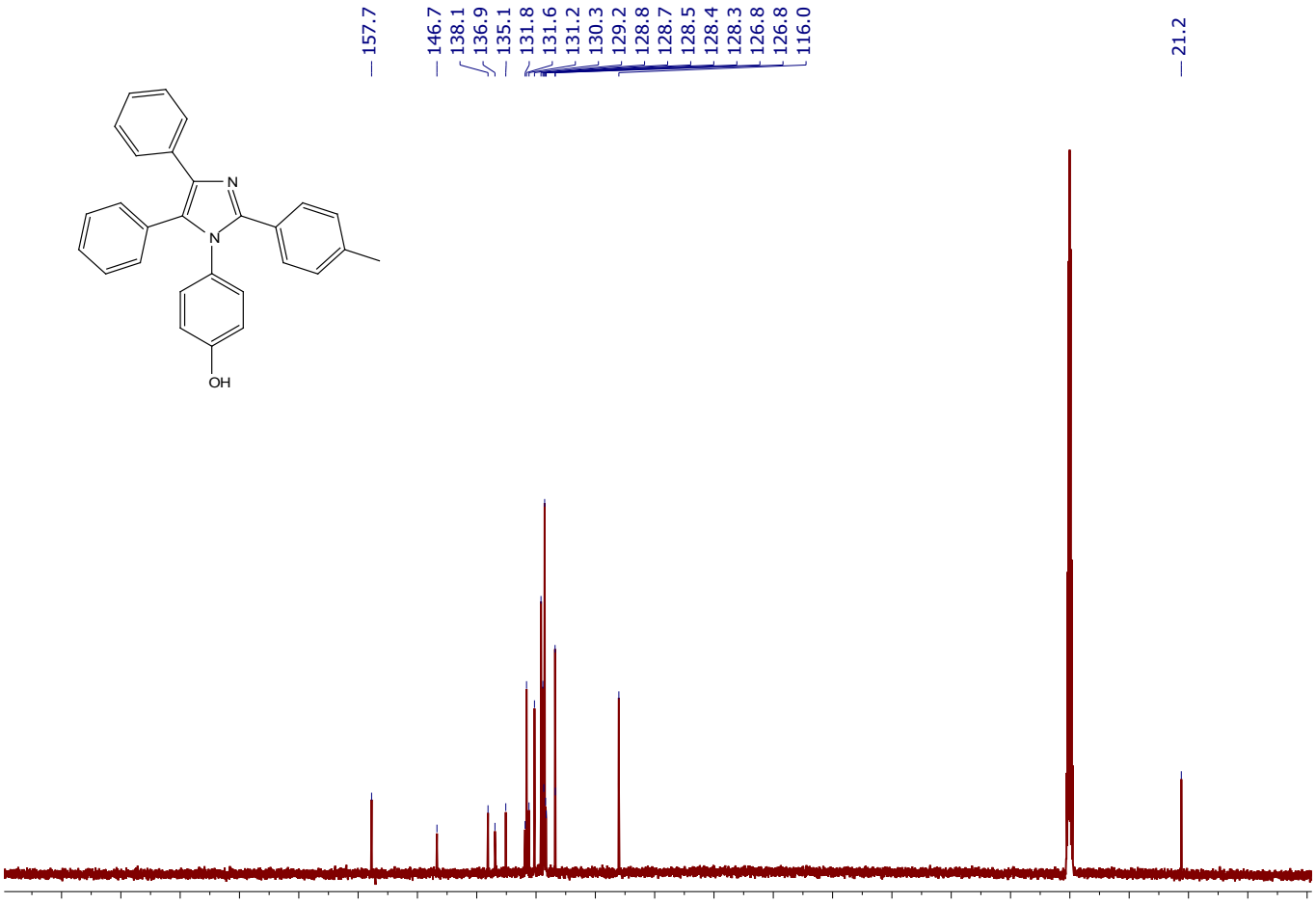

^{1}H, ^{13}C NMR spectrum of 1-(4-Hydroxyphenyl)-2-(4-bromophenyl)-4,5-diphenyl-1*H*-imidazole (IMI-17)

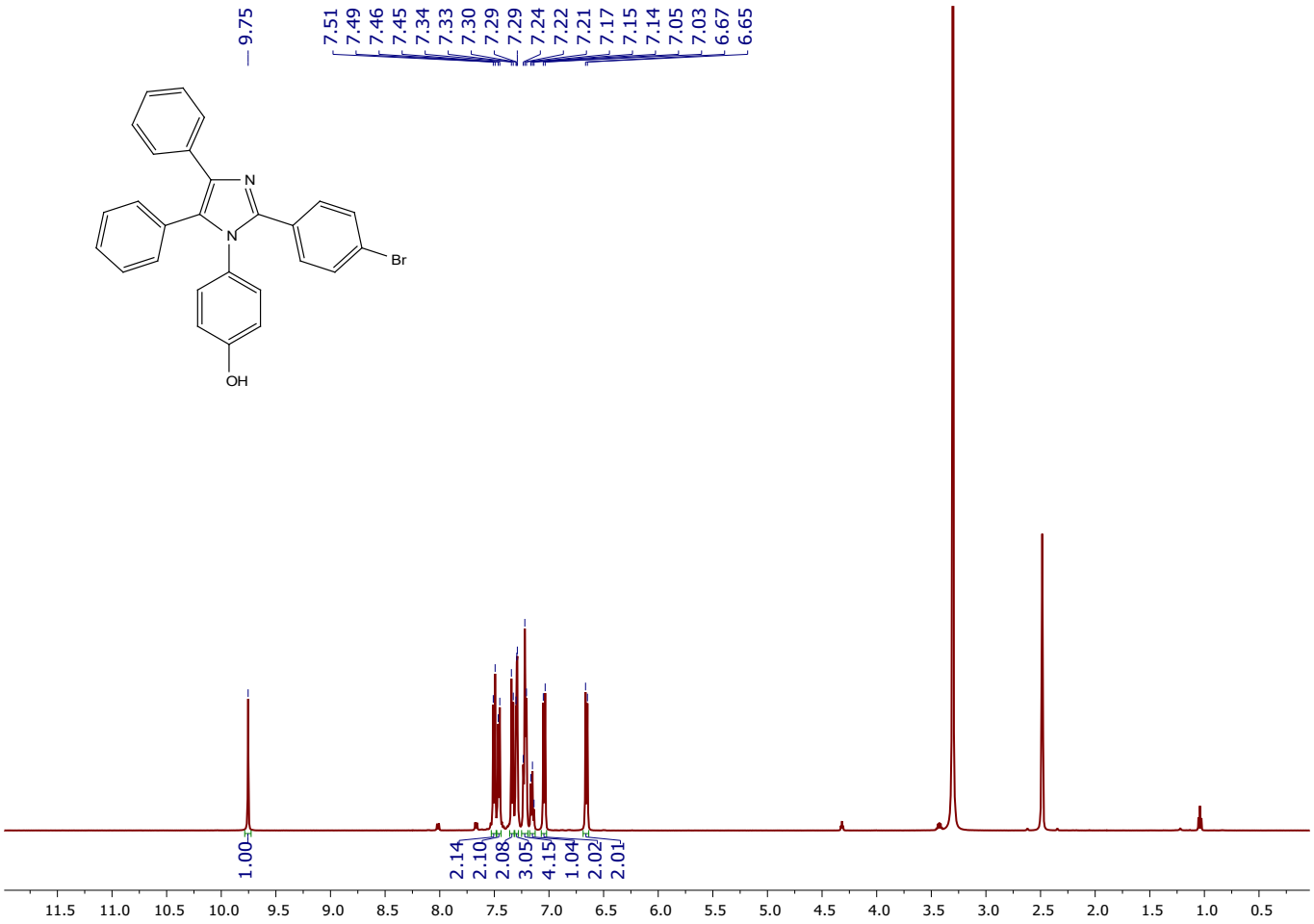

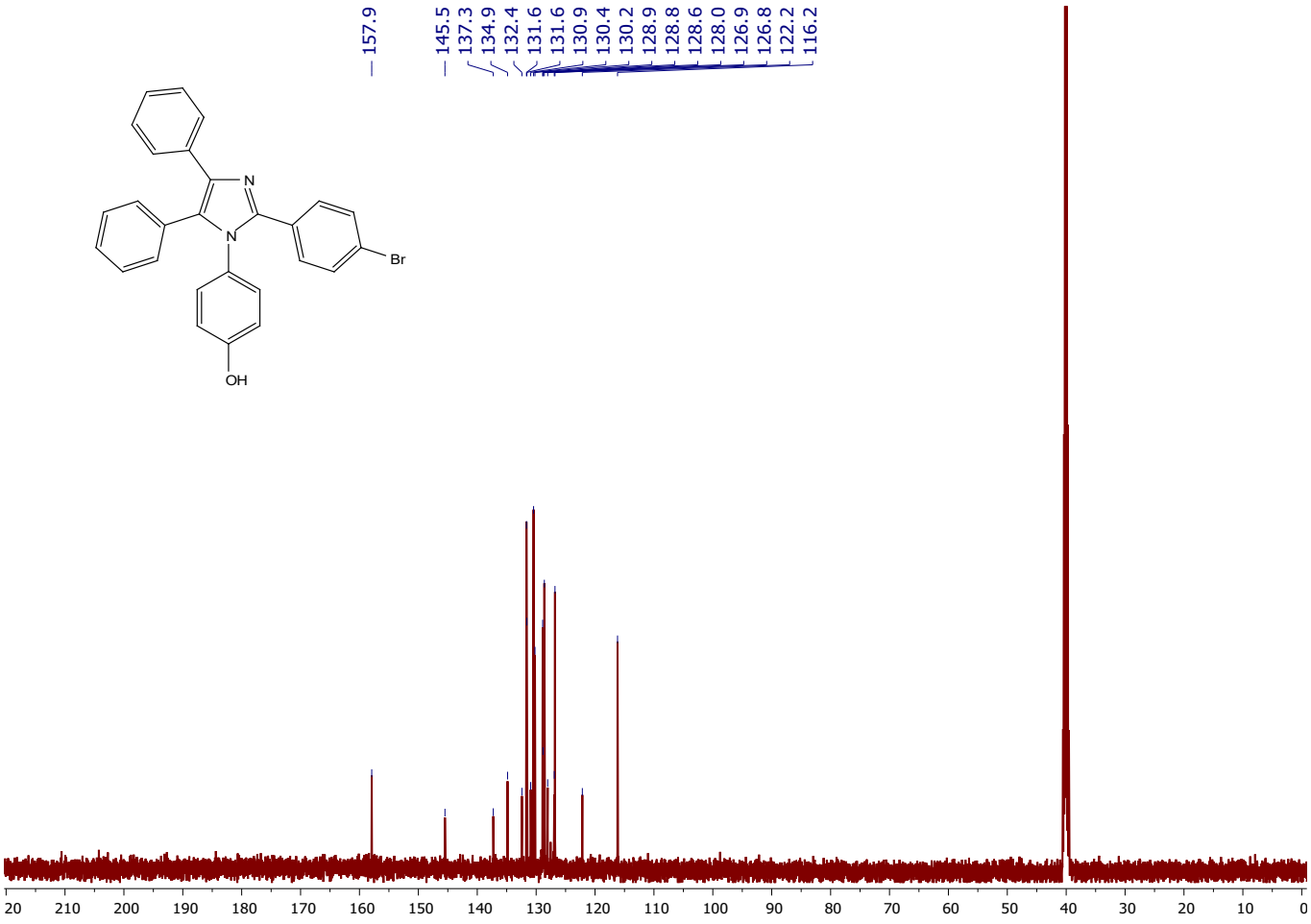

^{1}H, ^{13}C NMR spectrum of 1-(4-Hydroxyphenyl)-2-(4-fluorophenyl)-4,5-diphenyl-1*H*-imidazole (IMI-18)

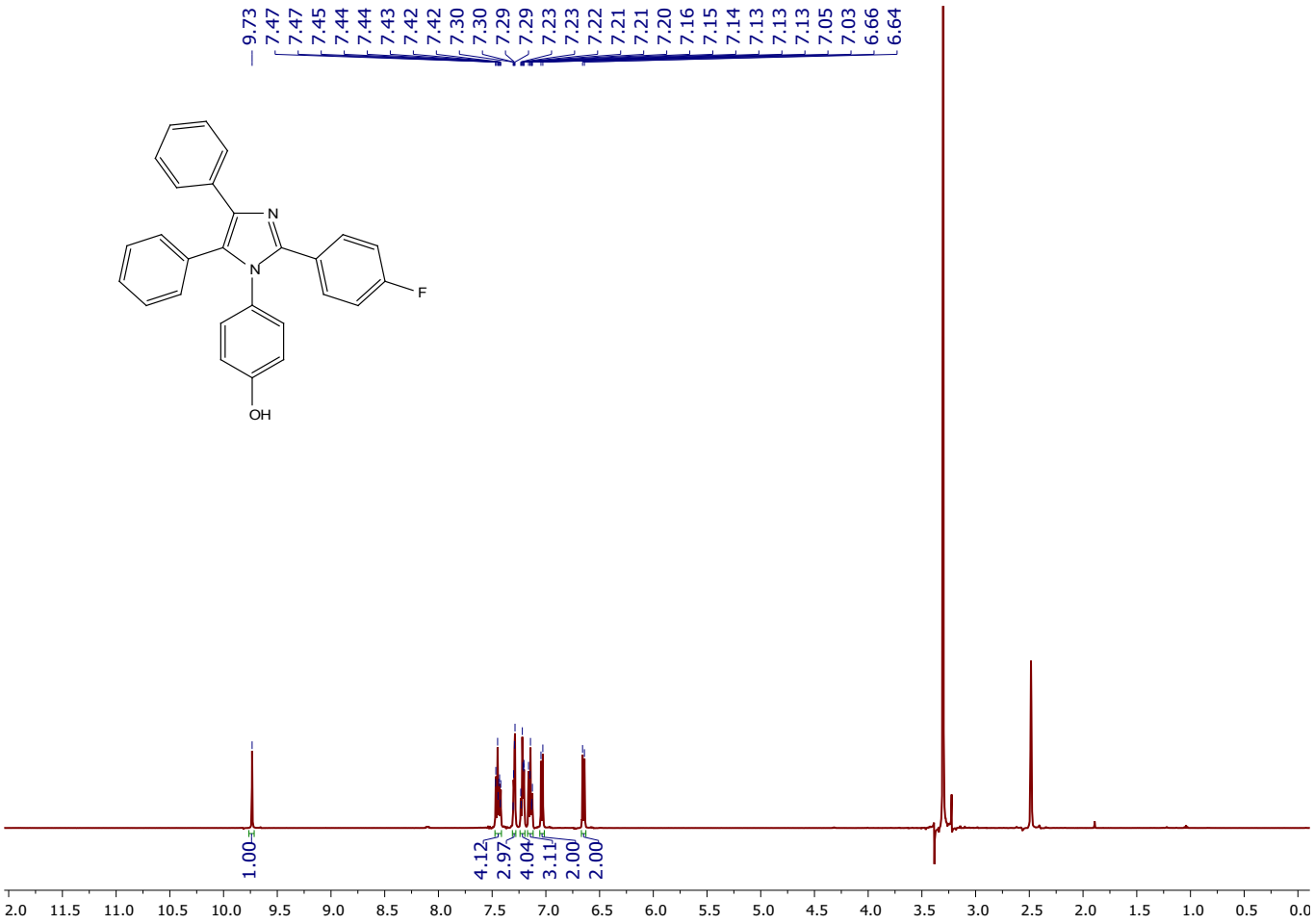

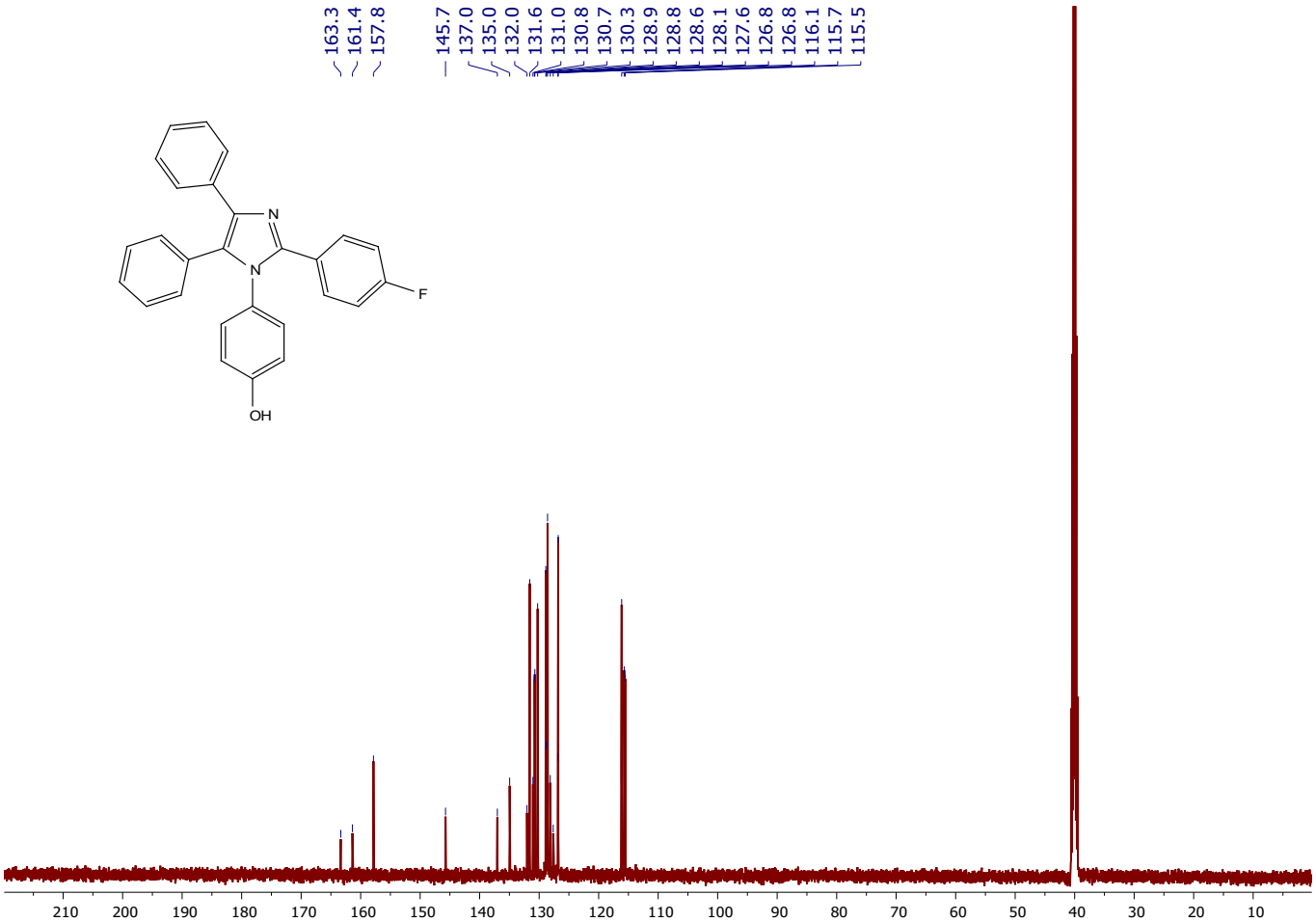

^{1}H, ^{13}C NMR spectrum of 1-(4-Hydroxyphenyl)-2-(4-methoxyphenyl)-4,5-diphenyl-1*H*-imidazole (IMI-19)

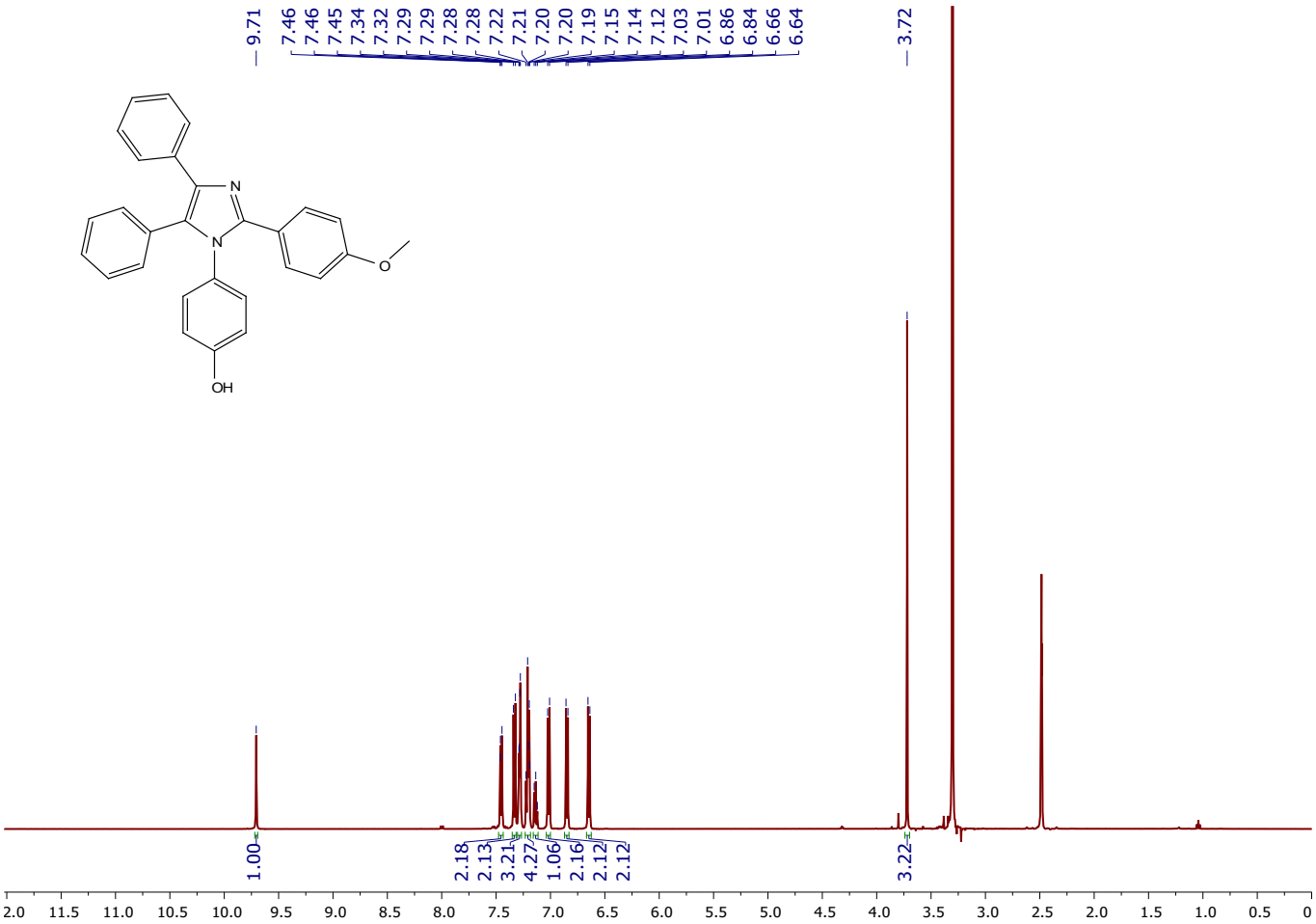

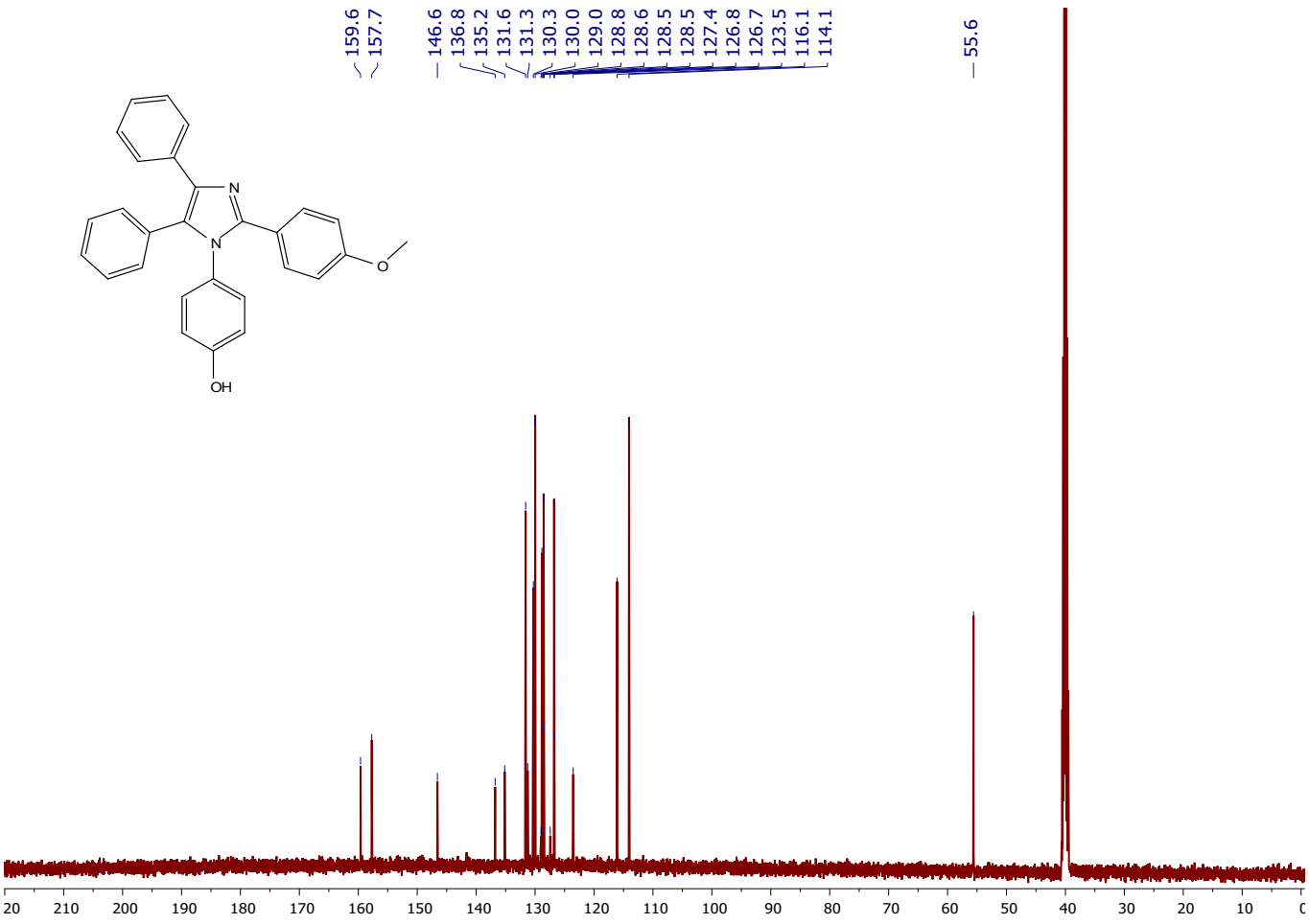

^{1}H, ^{13}C NMR spectrum of 1-(4-Hydroxyphenyl)-2-(4-(dimethylamino)phenyl)-4,5-diphenyl-1*H*-imidazole (IMI-20)

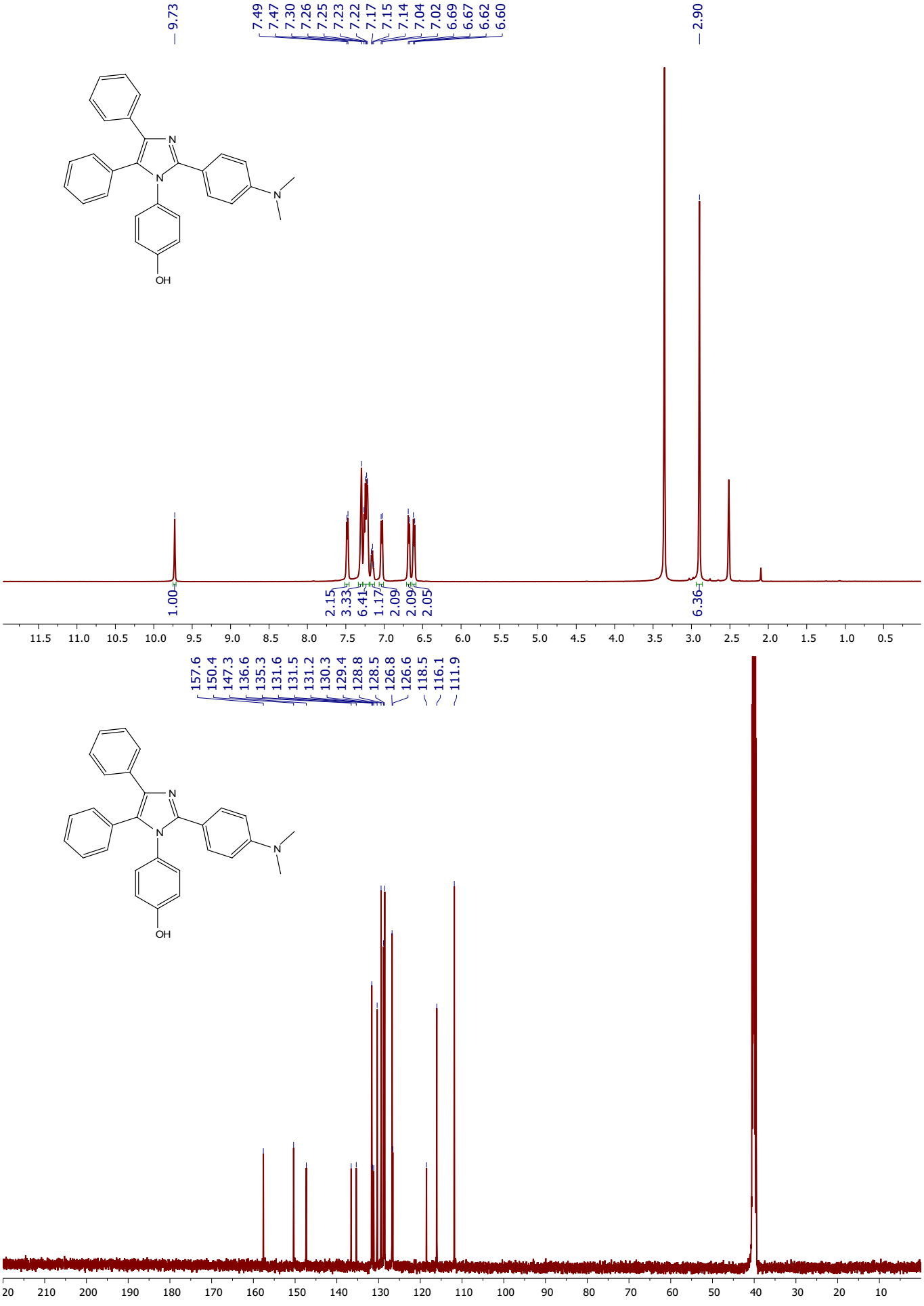

^{1}H, ^{13}C NMR spectrum and HRMS of 2-Cyclohexyl-1-(4-hydroxyphenyl)-4,5-triphenyl-1*H*-imidazole (IMI-21)

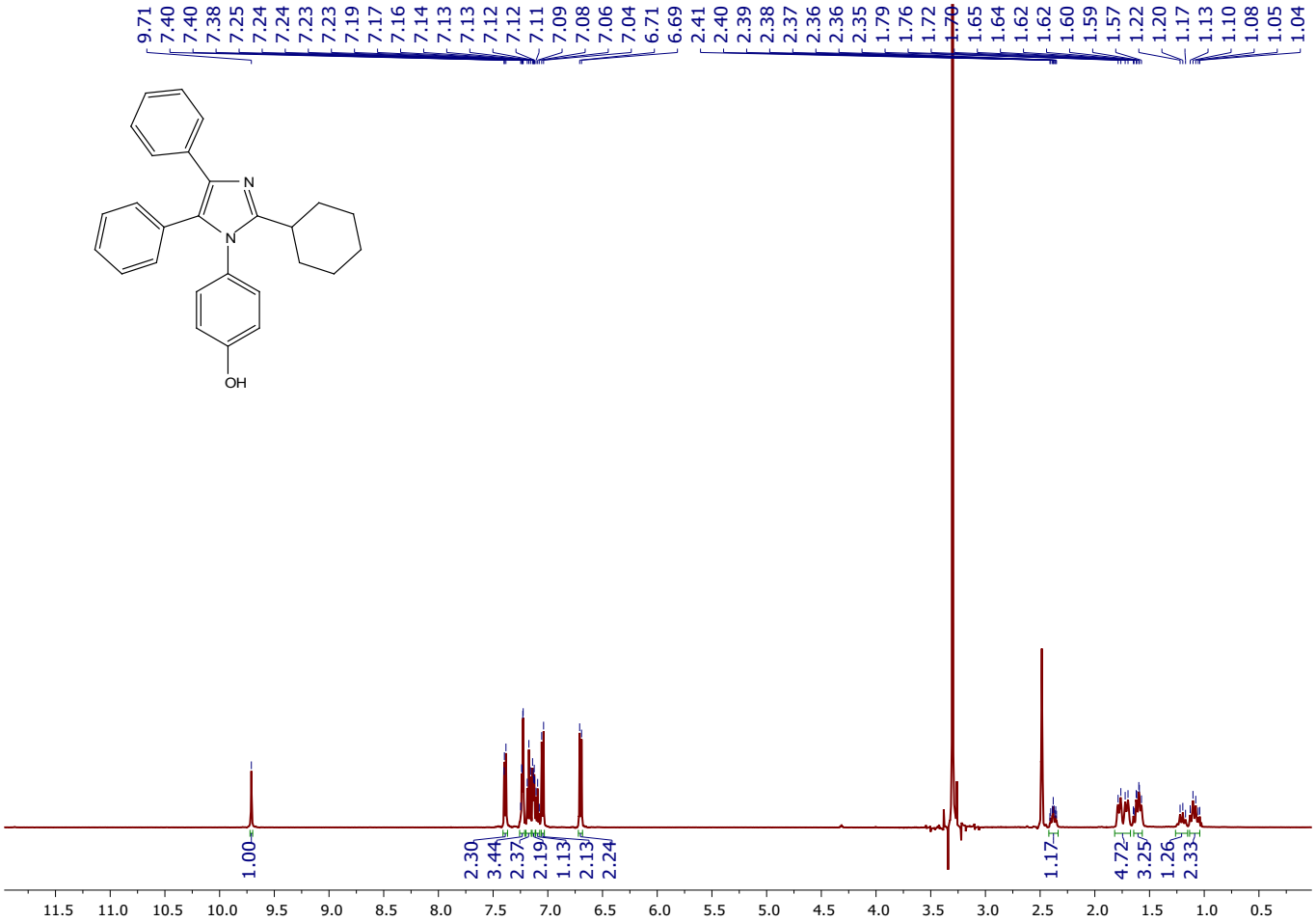

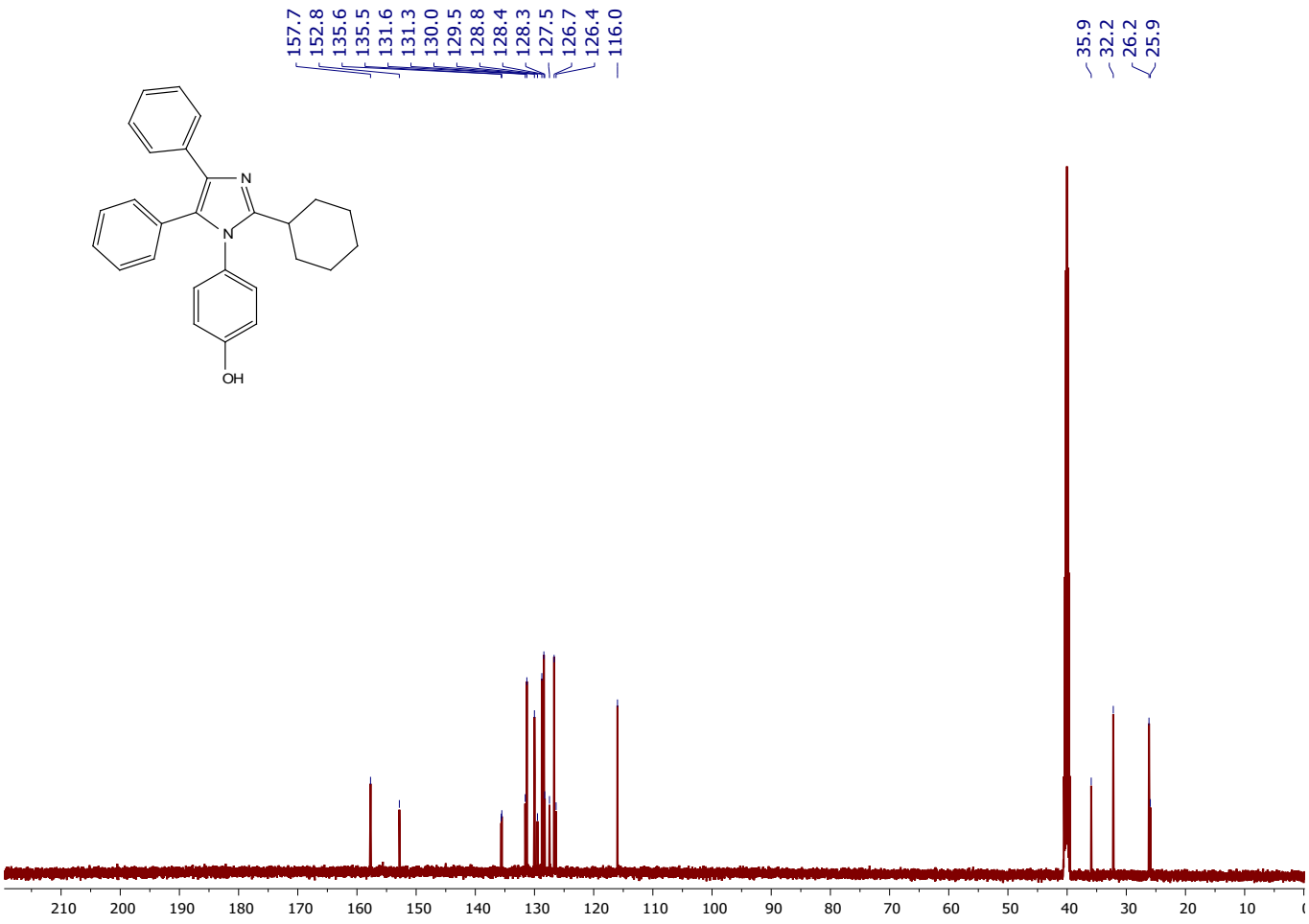

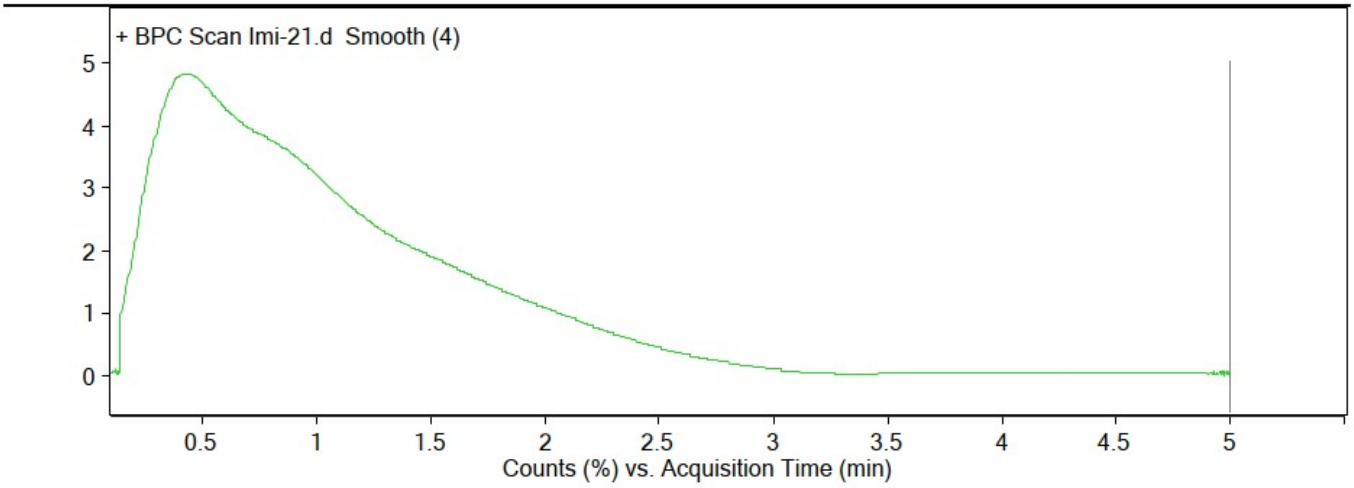

User Spectra

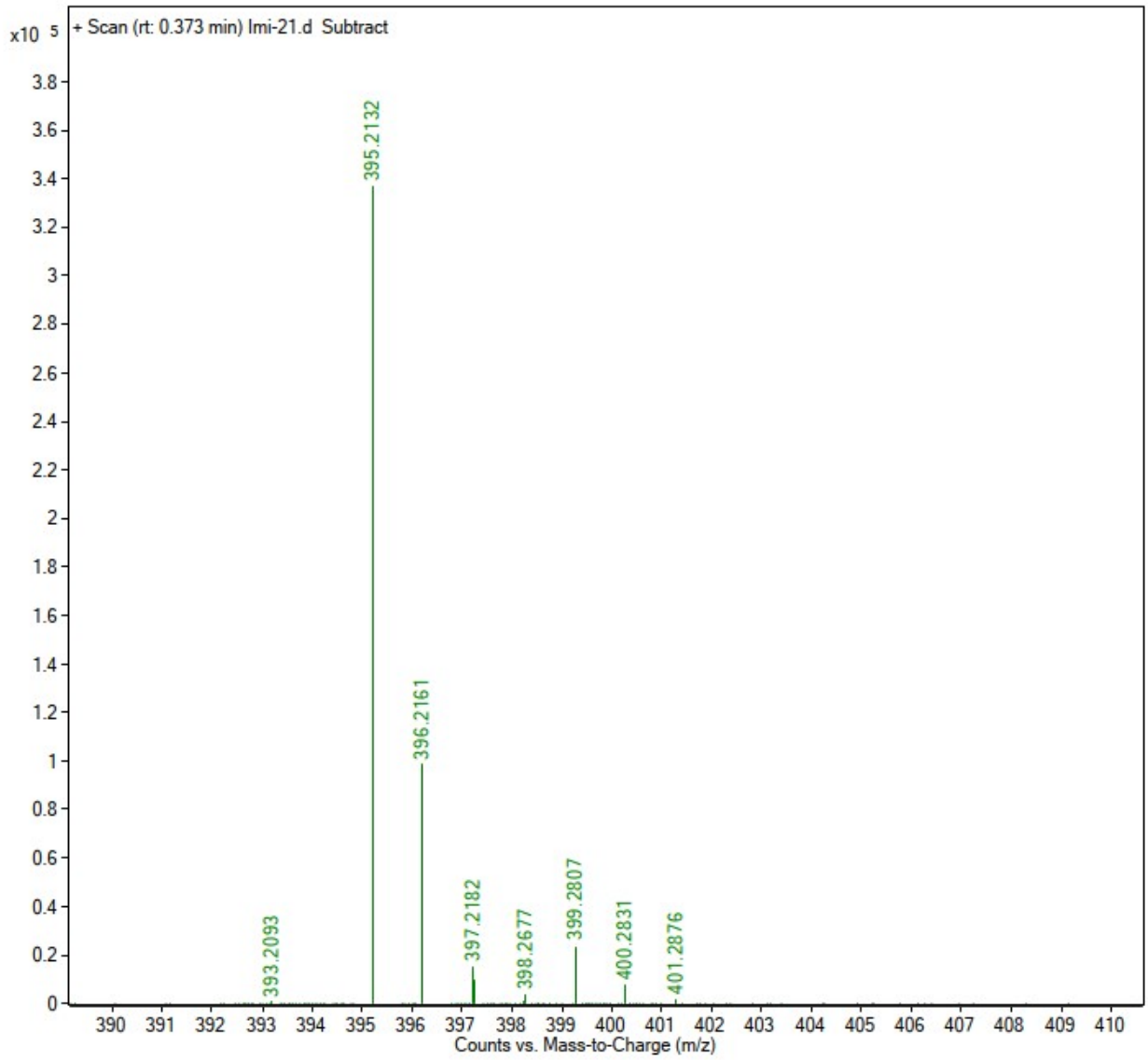

Section S6. References

1. S. U. Bhat, R. A. Naikoo and R. Tomar, *J Int. Res. J. Pure Appl. Chem*, 2016, **11**, 1-10.
2. A. Teimouri and A. N. Chermahini, *J Mol Catal A Chem.*. 2011, **346**, 39-45.
3. J. Safari and Z. Zarnegar, *C R Chim.*, 2013, **16**, 920-928.
4. B. Das, J. Kashanna, R. A. Kumar and P. Jangili, *Monatshefte für Chemie - Chemical Monthly*, 2013, **144**, 223-226.
5. M. P. Nadamani, N. O. Mahmoodi, M. Mamaghani, M. A. Zanjanchi and H. T. Nahzomi, *ChemistrySelect*, 2019, **4**, 8470-8476.
6. S. Samai, G. C. Nandi, P. Singh and M. S. Singh, *Tetrahedron*, 2009, **65**, 10155-10161.
7. A. R. Moosavi-Zare, Z. Asgari, A. Zare, M. A. Zolfigol and M. Shekouhy, *RSC Adv.*, 2014, **4**, 60636-60639.
8. J. Safari, S. Gandomi-Ravandi and Z. Akbari, *J. Adv. Res.*, 2013, **4**, 509-514.
9. K. Sivakumar, A. Kathirvel and A. Lalitha, *Tetrahedron Letters*, 2010, **51**, 3018-3021.
10. H. V. K. Nagaraja Naik, J. Rangaswamy, S.T. Harinia and T.C. Umeshkumar, *J. Appl. Pharm. Sci.*, 2012, **2**, 67-74.
11. K. D. Safa, A. Feyzi, M. Allahvirdinesbat, L. Sarchami and P. N. Panahi, *Synth. Commun.*, 2015, **45**, 382-390.
12. K. D. Safa and H. Mousazadeh, *Synth. Commun.*, 2016, **46**, 1595-1604.
13. H. V. K. Nagaraja Naika, J. Rangaswamya, S.T. Harinia and T. C. Umeshkumara, *Three component one pot synthesis of 5-Substituted 1-Aryl-2,3-diphenyl imidazoles: A novel class of promising antioxidants %J Journal of Applied Pharmaceutical Science*, ssue: 11.
14. G. Sharma, A. Sain, N. Kumar and D. Pathak, *Indian J. Heterocycl. Chem.*, 2010, **19**, 311-312.
15. K. D. Safa, M. Allahvirdinesbat, H. Namazi and P. N. Panahi, *Comptes Rendus Chimie*, 2015, **18**, 883-890.
16. K. D. Safa, L. Sarchami, M. Allahvirdinesbat, A. Feyzi and P. N. Panahi, *Journal of Chemical Research*, 2014, **38**, 571-576.
17. N. Naik, *Journal of Applied Pharmaceutical Science*, 2012, DOI: 10.7324/JAPS.2012.21112.
18. Z. Ghasemi, A. Mirzaie, R. Arabzadeh, Z. Fathi and A. Abolghassemi Fakhree, *Journal of Chemical Research*, 2019, **43**, 262-267.
19. K. D. Safa, M. Allahvirdinesbat and H. Namazi, 2015, DOI: 10.6084/m9.figshare.1311742.v4.